12

Jupiter's Outer Satellites and Trojans

David C. Jewitt
Institute for Astronomy, University of Hawaii

Scott Sheppard
Institute for Astronomy, University of Hawaii

Carolyn Porco
Southwest Research Institute

12.1 INTRODUCTION

Jupiter's irregular satellites possess large, eccentric and highly inclined orbits. They are conventionally considered separately from the temporarily captured satellites and the Trojans (the latter co-orbiting the Sun leading and trailing Jupiter by 60 deg). However, there is reason to believe that objects in these three groups share many similarities, both in terms of their physical properties and their origins. Accordingly, in this review we jointly discuss the irregular and temporary satellites and the Trojans.

In the modern view of the solar system, different populations of small bodies can be traced back to their origin in the protoplanetary disk of the Sun. Most planetesimals that formed near the orbits of the giant planets were promptly ejected from the planetary region. A small fraction of those ejected (perhaps 10%) remain bound to the Sun in the $\sim 10^5$ AU scale Oort Cloud which provides a continuing source of the long-period comets. Planetesimals growing beyond Neptune were relatively undisturbed and their descendants survive today in the Kuiper Belt. The Kuiper Belt in turn feeds the giant-planet crossing Centaurs, which are then converted by planetary (largely Jovian) perturbations into Jupiter Family Comets (JFCs; short-period comets which are strongly interacting with Jupiter, formally those with Tisserand invariants $2 \leq T \leq 3$). During their interaction with Jupiter, the comets sometimes become temporarily trapped. Main-belt asteroids near resonances with Jupiter can also be excited into Jupiter-crossing orbits, and may contribute to the populations of temporarily trapped objects. Since there is currently no effective source of energy dissipation, neither the temporary satellites nor the Trojan librators can be captured as permanent members of these populations. Temporary members will be either flung out of the Jovian system or impact the planet or one of the Galilean satellites. However, at very early epochs, at the end of Jupiter's $\leq 10^6$ to $\leq 10^7$ yr growth phase, several mechanisms might have operated to permanently trap objects from these and other reservoirs. Therefore, populations which are not now interacting may once have been so. Given the dynamical interrelations (Figure 1), it is to be expected that the physical and compositional natures of the various bodies should be related.

Figure 1: Interrelations among the populations considered in this chapter. Solid arrows denote established dynamical pathways. At the present epoch, in which sources of energy dissipation are essentially absent, no known pathways (dashed lines) exist between the temporary and permanent satellite and Trojan populations. Numbers in parentheses indicate the approximate dynamical lifetimes of the different populations.

The irregular satellite and the Trojan populations both became known about 100 years ago from early photographic surveys. The first irregular satellite, JVI Himalia, was discovered photographically in 1904 (Perrine 1905). Additional members have been slowly added to this group throughout the 20th Century (Figure 2). The photographic surveys and the implied limits to completeness are well described in Kuiper (1961), while a later photographic survey was reported by Kowal et al. (1978). A second wave of discovery, driven by the use of large format charge-coupled devices (CCDs) to survey the near-Jupiter environment, is underway. The number of known irregular Jovian satellites jumped from 8 to 50 (as of April 2003) within the last 3 years (Sheppard et al. 2001, 2002). In this review, however, we confine our attention to the 32 having well determined orbits.

The first Trojan, 588 Achilles, was recognized in 1906 in a separate photographic observation by Max Wolf in Heidelberg (Wolf 1906). Later wide field photographic (van Houten et al. 1991) and CCD surveys have further increased the sample. The currently known Trojan population exceeds 1200 (Figure 2).

Figure 2: Known populations of the Jupiter irregular satellites (solid line) and Trojans (dashed line) as a function

of date. Both populations became known at the start of the 20th century, as a result of the application of photographic imaging. The surge in the known populations towards the end of the century results from new imaging surveys using wide-field charge-coupled devices.

Information on the small objects in the Jupiter system has been obtained almost entirely from ground-based observations. The main spacecraft observations include a series of Voyager 2 images of the second largest outer irregular satellite, JVII Elara, and a series of resolved images of the largest irregular, JVI Himalia, taken by the Cassini cameras (Figure 3) during that spacecraft's Jupiter flyby in late 2000 (Porco et al. 2003). The Trojans have yet to be visited by any spacecraft.

Figure 3: The disk of Himalia illuminated from the left at a phase angle of 70 deg. and observed by the Cassini ISS over ~4.5 hours. One unprocessed image from each of four observation sequences is shown in the top row. The observation times were (from left to right): 18 December 2000, 20:30 UTC, 22:00 UTC, 23:30, UTC, and 19 December 2000, 01:04. The bottom row shows the same data, but smoothed by bicubic interpolation. Figure from Porco et al (2003).

Irregular satellites are known around the other gas giants. Saturn, Uranus and Neptune have 13, 6 and 4 (or 5, if Triton is so counted), respectively (Kuiper 1961, Gladman et al. 2000, 2001, Holman et al. 2003). A single Trojan (2001 QR322) has been detected in association with Neptune and simulations suggest that such objects should be dynamically stable on 10^7 year timescales and longer around all four giant planets (e.g. Holman and Wisdom 1993, Nesvorny and Dones 2002). Another type of 1:1 resonance, in which the object librates around the longitude of the associated planet, has also been found to be long-lived at Uranus and Neptune but not at Jupiter or Saturn (Weigert, Innanen and Mikkola 2000). No such "quasi-satellites" have yet been detected.

The irregular satellites have been previously reviewed by Cruikshank, Degewij and Zellner (1982). The Trojans were previously reviewed by Shoemaker, Shoemaker and Wolfe (1989), while their physical properties have been more recently discussed by Barucci et al. (2003). The temporary satellites have been recognized as a group for some decades but have not been extensively discussed in the literature. They are important both for the clues they provide about the dynamics of capture and because we possess compelling examples of temporary satellites that interact with the Jovian system in interesting ways (e.g. the Jupiter-impacting comet D/Shoemaker-Levy 9: see chapter by Harrington et al.). In this review, we discuss the nature of, origin of and interrelations among this collection of bodies.

12.2 THE IRREGULAR SATELLITES

The irregular satellites of Jupiter occupy orbits that are large, eccentric and highly inclined relative to those of the regular system (the Galilean satellites and attendant small inner bodies: for the latter, see the chapter by Burns et al.). A majority of the known examples are retrograde (inclination $i \geq 90$ deg.; Table 1) and they reach vast jovicentric distances (up to 474 R_J (0.22 AU) for the apojove of JXIX). For comparison, Jupiter's region of gravitational control extends out roughly to the edge of the Hill sphere, of radius

$$r_H = a_J \left(\frac{m_J}{3(m_J + m_\odot)} \right)^{1/3} \quad (1)$$

where a_J and m_J are the orbital semi-major axis and the mass of Jupiter, respectively, and $m_\odot$ is the mass of the Sun. With $m_J/m_\odot \sim 10^{-3}$ and $a_J = 5$ AU, we obtain $r_H \sim$ 0.35 AU (735 R_J), corresponding to an angular radius of 5 degrees when viewed at opposition from the Earth. The semi-major axes of the known irregular satellites extend out to about 0.5 r_H and, as of January 2003, their total number stands at 50 (the 32 with well-determined orbits are listed in Table 1). However, this is a strong lower limit to the intrinsic population because observational coverage of the Hill Sphere is incomplete and because many smaller irregulars remain undetected. The fraction of the Hill sphere that has been searched for Jovian satellites is a function of the survey limiting magnitude. For apparent V-band (0.55 μm) magnitude $m_V \leq 20$, the coverage is probably close to complete over the whole Hill Sphere, although even this assertion is difficult to justify given the lack of documentation regarding past satellite surveys, particularly those conducted photographically. In our own work, only $\sim 25\%$ of the Hill Sphere has yet been examined to a limiting red (0.65μm wavelength) magnitude $m_R \sim 23.5$.

For objects at Jupiter's distance and at opposition, m_V, and diameter, D [km], are approximately related through

$$m_V = 25.73 - 5log(D) - 2.5log\left[\frac{p_V}{0.04}\right] \quad (2)$$

where p_V is the V-band geometric albedo. We take p_V = 0.04 (Cruikshank 1977), which means that the deeper satellite surveys (limiting magnitude $m_V \sim 23.5$), can detect satellites of diameter $\sim$ 2.8 km. The largest irregular satellite, JVI Himalia, is aspherical with an effective circular diameter of roughly 150 km (Cruikshank 1977, Porco et al. 2003). The smallest known irregular satellites have effective diameters of order 2 km (Table 1). Presumably, much smaller satellites exist: the timescales for orbit decay by Poynting-Robertson and plasma drag exceed the age of the solar system for diameters in excess of a few centimeters.

The irregular satellites are extremely susceptible to solar perturbations, particularly when near apojove. Large retrograde orbits are more stable against these perturbations than prograde orbits (Henon 1970) consistent with the observation that the most distant satellites are all retrograde. This also suggests that the current satellites are survivors of a once larger population that has been progressively depleted due to dynamical instabilities. Kozai (1962) considered the effect of time-averaged solar perturbations on the motion of a planetary satellite. He found that the normal component of the satellite angular

momentum is conserved, such that variations in eccentricity and inclination must be correlated. Satellites which develop high inclinations in response to external forcing also acquire high eccentricities. The resulting small perijove and apojove distances render these satellites susceptible to collision with Jupiter or the Galilean satellites or, more usually, to escape from the Hill sphere. Long term (10^9 yr) integrations reveal a zone of depletion at inclinations $55 \leq i \leq 130$ deg caused by solar and planetary perturbations that drive the perijoves of satellites to small values (Carruba et al 2002). For a satellite with perijove inside the region of the Galileans, the probability of collision per orbit is roughly given by $P \sim (r_s/2R_s)^2$, where r_s and R_s are the Galilean satellite physical radius and orbital radius, respectively. Taking Callisto as an example, with $r_s \sim 2400$ km and $R_s \sim 23\ R_J$, we obtain $P \sim 5 \times 10^{-7}$. Highly eccentric satellite orbits with periods $\tau \sim 1$ yr would survive for only $\tau/P \sim 2 \times 10^6$ yrs before colliding with or being scattered by the Galileans. For this reason, it is not surprising that the known irregular satellites completely avoid the Galileans: the smallest perijove is 80 R_J, for JXVIII. The long term stability of orbits exterior to the Galilean satellites but interior to the innermost known irregulars has not been explored. In some models, this region would have overlapped with the outer parts of the disk which seeded the growth of the Galilean satellites. Detection of surviving bodies here would be particularly interesting.

Figure 4: Orbital semi-major axis (in R_J) vs. eccentricity, for the Jovian irregular satellites. The symbols are coded for satellite size, computed from assumed 0.04 albedos, as indicated.

The orbital elements of the irregular satellites are non-randomly distributed. We name the dynamical groups after the largest known member of each (Sheppard and Jewitt 2003). The Themisto (semimajor axis $a \approx 105\ R_J$, inclination $i \approx 43$ deg.) and Himalia ($a \approx 160\ R_J$, $i \approx 28$ deg) groups are prograde (Table 1). Themisto is currently the only known member of the former group, while five Himalias have been detected. The many retrograde satellites show evidence for division into at least three groups named for Ananke ($a \approx 295\ R_J$, $i \approx 148$ deg), Pasiphae ($a \approx 325\ R_J$, $i \approx 152$ deg) and Carme ($a \approx 325\ R_J$, $i \approx 165$ deg, see Figures 4 and 5). The satellites within each group may be fragments produced by collisional shattering of parent bodies (Kuiper 1956, Pollack, Burns and Tauber 1979). If so, the individual satellite clusters should be regarded as analogues of the dynamical families found amongst the main-belt asteroids. Many properties of the asteroid families are still not well established but it is instructive to attempt a comparison between them and the irregular satellite groups. The size distributions offer one basis for comparison.

The size distributions of the asteroid families are sharply peaked, with the largest bodies probably consisting of gravitationally reaccumulated blocks produced after catastrophic failure of the target body (Michel et al. 2001). Very roughly, the size distributions can be represented by differential power laws

$$n(r)dr = \Gamma r^{-q} dr \tag{3}$$

in which $n(r)dr$ is the number of objects having radius between r and $r + dr$ and Γ and q are constants. The size distributions, of both real dynamical families (Tanga et al. 1999) and numerical model families (Michel et al. 2001), are compatible with $q \geq 3$. This compares with the $q \sim 3$ size distribution of the non-family asteroids and the $q \sim 3.5$ index produced by an equilibrium cascade, in which particles are progressively shattered to smaller and smaller fragments (Dohnanyi 1969).

Figure 5: Orbital semi-major axis (in R_J) vs. inclination, for the Jovian irregular satellites. The symbols are coded for satellite size, computed from assumed 0.04 albedos, as indicated.

Figure 6: Cumulative luminosity function of the irregular satellites. Different symbols show the data and data corrected for survey inefficiencies. The straight line has a slope corresponding to a $q = 2$ power law.

The irregular satellite cumulative luminosity function (number of satellites brighter than a given apparent magnitude) is shown in Figure 6, based on our survey observations on Mauna Kea. The satellites are best fit by $q \sim 2$ over the magnitude range $14 \leq m_R \leq 18.5$ (approximate diameter range $20 \leq D \leq 180$ km), while asteroid-like size distributions steeper than $q = 3$ are inconsistent with the data. This observation suggests that, if the irregular satellites are members of collisionally produced families, some other process has acted to modify the post-breakup size distribution (c.f. Gehrels 1977). One possibility is that the smaller irregular satellites have been preferentially removed by gas drag in an early extended Jovian atmosphere, as we discuss below. The size distribution at $m_R > 18.5$ is less well determined. Our best estimates of the correction for survey sky-plane incompleteness suggest a depletion relative to the $q = 2$ distribution (Figure 6). It is also true that the mass within each of the five satellite groups is dominated by the largest member. In the context of collisional disruption this suggests formation by impacts with energies barely above the disruption threshhold, allowing gravitational reaccumulation of many fragments into the largest object.

Physical observations provide a second basis for comparison of the satellite groups with the asteroid families. As in the main belt, there is hope that close examination of the fragments might provide a glimpse of the interior structure of the parent body. For example, differentiated asteroids should, upon disruption, produce fragments consisting of core (nickel-iron), mantle (olivine) and crustal (silicate) materials. The satellites, with their presumed rock-ice composition, might fragment into low-density (icy) and high density (rocky) components. These expectations in the main belt at first seemed borne-out by colorimetric and spectroscopic data, but recent measurements have shown that compositional differences among family members are muted, and much smaller than the full compositional range observed in the main belt. Objects originally identified

as metallic core fragments, for instance, seem not to be metallic upon subsequent examination (see discussion in Bus 1999). The implications of this observational result are not clear.

Figure 7: Optical colors of the eight brightest irregular satellites, from Rettig (2001).

Evidence from physical observations of the satellites is limited. The colors of the satellites range from neutral ($V - R \sim 0.35$, the color of the Sun on the Johnson-Kron-Cousins system) to moderately red ($V - R \sim 0.50$, Luu 1991). The satellites generally lack the ultra-red material found on the Centaurs and Kuiper Belt Objects (Jewitt and Luu 2001, Jewitt 2002). In the optical, Rettig et al. (2001) and Grav et al. (2003) find that the bright retrogrades are redder and less uniform in color than the bright progrades (Figure 7). This may be because the retrograde objects belong to several discrete families, each with different parents, whereas the measured prograde satellites are all from the Himalia group and share a common parent. Sykes et al. (2000) used near infrared photometry to find that the retrograde satellites (other than JXII Ananke) are systematically redder than the prograde satellites and suggested that the retrogrades are fragments of a D-type body while the progrades result from breakup of a C-type. The available color observations are consistent with the breakup of a single object of internally uniform composition to form the prograde Himalia group (JVI, JVII, JX and JXIII). The wider dispersion among the colors of the retrograde satellites may suggest more than one parent body, as suggested in the scatter of the a-i and, to a lesser extent, a-e plots (Figures 4 and 5). The least arguable conclusion is that many more observations are needed to define and interpret color systematics in the irregular satellites.

Figure 8: Time-resolved optical reflection spectra of JXII Ananke. The spectra have been carefully normalized to the spectrum of the Sun, and are vertically offset from one another for clarity. Each spectrum is marked by the Universal Time and date on which it was taken. Figure provided by Jane Luu.

Jarvis et al. (2000) reported weak 0.7 μm absorption in the optical spectrum of JVI Himalia and attributed this to an Fe^{2+} to Fe^{3+} transition in phyllosilicates. This latter material is typically produced by aqueous alteration, requiring the presence of liquid water for an extended period of time. The Jarvis et al. spectra show an optically blue object from which spectral class F is assigned. Since most F-types are found in the main belt, they speculate that JVI Himalia is a captured main-belt object. However, the magnitude of the spectral slope in their data appears to vary from night to night: rotational modulation caused by compositional variations is a possible explanation. Their spectra appear inconsistent with broadband (ECAS) photometry of Tholen and Zellner 1984. The near infrared ($1.4 - 2.4\mu m$) spectrum of JVI Himalia is featureless and specifically lacking the $1.5\mu m$ and $2.0\mu m$ water ice bands (Geballe et al. 2002). A marginal detection of the deeper $3\mu m$ water ice feature has been recently reported (Brown et al. 2002). The $1.4 \leq \lambda \leq 2.4\mu m$ spectra of JVII Elara and JVIII Pasiphae are featureless. Small but probably significant rotational variations in optical spectral gradient are seen in JXII Ananke (Figure 8).

12.2.1 Irregular Satellites of Other Planets

Irregular satellites have also been detected at Saturn (13, the largest being 110 km radius Phoebe), Uranus (6) and Neptune (5, including Triton) but are not known to be associated with any of the (much less massive) Terrestrial planets. At the vast distances of the outer planets, only the larger irregulars can be easily detected and the known populations are correspondingly smaller and less well characterised than at Jupiter. Conversely, it is easier to search the entire Hill spheres of the more distant planets than at Jupiter, so that meaningful estimates of population completeness are possible. Some properties are found in common with those of the Jovian irregulars, including evidence for inclination clustering in the Saturn and Uranus systems that is suggestive of an origin by fragmentation of a small number of parent bodies (Gladman et al. 2001, Sheppard and Jewitt 2003).

Their distended nature leaves the irregular satellite systems susceptible not only to external perturbations from the Sun, but potentially also from other heliocentric bodies. Beauge et al. (2002) have explored the interaction between the irregular satellites and the circumsolar disk. They find that the planetary migration inferred to explain the population of Kuiper Belt Objects trapped in the 3 : 2 mean motion resonance with Neptune would have had a disruptive effect on the irregulars of this planet and of Uranus.

12.2.2 Origin of the Irregular Satellites

No plausible models exist to explain the large, highly eccentric and inclined (including retrograde) orbits of the irregular satellites by accretion in a bound, circum-Jovian nebula. Instead, the irregular satellites must have been formed elsewhere and then captured by Jupiter. The existence of the dynamical groupings (Figures 4 and 5) argues that the current satellites are fragments of precursor objects (Kuiper 1956), but it is not clear whether fragmentation occurred as part of the capture process, or was a product of later, unrelated bombardment by the flux of interplanetary projectiles. The latter seems more plausible given that the velocity dispersion imparted to fragments by aerodynamic forces is small compared to the escape velocity of satellites as large as Himalia or Pasiphae.

Jupiter can capture nearby objects by at least three mechanisms. Temporary libration point capture is possible when a body moving in heliocentric orbit approaches Jupiter through its L1 Lagrangian point at less than about 1% of the orbital velocity of Jupiter (Heppenheimer and Porco 1977). In the absence of energy dissipation, the capture is fully reversible and temporary satellites leak out through L1 after a small number of orbits about the planet (Heppenheimer and Porco 1977, Benner and McKinnon 1995). For an object to be captured by a fixed-mass Jupiter from heliocentric orbit requires the dissipation of energy. Frictional dissipation in the extended envelope of proto-Jupiter

has been suggested (Heppenheimer and Porco 1977; Pollack, Burns and Tauber 1979), as has dissipation by collision with pre-existing satellites near Jupiter (Columbo and Franklin 1971). Regardless of the specific form of the dissipation, the capture of the irregular satellites must have occurred very early: Jupiter's extended gas envelope collapsed within the first million years after formation while the density of planetesimals near Jupiter was high enough for collisions to be probable only during the planet formation phase (perhaps lasting a few million years after Jupiter's envelope collapse).

The lifetime of a satellite orbiting within a gas of density ρ $[kg\ m^{-3}]$ is roughly given by the time needed for the satellite to intercept its own mass in gas. For a spherical satellite of diameter D, neglecting numerical factors of order unity the gas drag lifetime, τ_d, is given by

$$\tau_d \approx \left(\frac{\rho_s}{\rho}\right)\left(\frac{D}{C_d \Delta V}\right) \quad (4)$$

where ρ_s is the density of the satellite, $C_d \sim 1$ is the drag coefficient, and ΔV is the relative velocity of the satellite through the gas. Objects larger than a critical maximum size cannot be significantly retarded by drag within the lifetime of the gas envelope. Conversely, objects smaller than a certain minimum size can be stopped by gas drag: their fate is to spiral out of orbit into the body of the planet (Pollack et al. 1979). Indeed, gas drag has been suggested as a mechanism by which the ice giant planets Uranus and Neptune might have accreted much faster than otherwise possible (Brunini and Melita 2002). Gas drag sufficient to enable capture could also lead to modification of the size distribution of the fragments between these extremes, reducing the power law index and truncating the size distribution below a critical diameter. An observational assessment of the minimum satellite size has yet to be made, but the shallow size distribution is at least qualitatively consistent with the action of gas drag. Friction from gas drag should also lead to orbit circularization, on a timescale given by Eq. (4). Figure 4 shows that the largest satellites in each group have eccentricities higher than the respective mean eccentricities of the smaller members, qualitatively consistent with the action of drag, but the effect is not statistically significant.

Another form of capture of bodies from adjacent heliocentric orbits could occur if Jupiter's mass were to suddenly increase (or, equivalently, the Sun's mass were to suddenly decrease) by a large factor, leading to rapid expansion of the Hill sphere (Eq. (1), Heppenheimer and Porco 1977). This so-called "pull-down" capture, which favors retrograde satellites, requires the mass to change on timescales comparable to the crossing time of the Hill sphere, perhaps only a few years. Unlikely as this seems, some models of Jupiter's formation indeed predict very rapid mass growth. Provided mass is added isotropically to Jupiter, the change in the satellite orbit radius, a, is given by (Jeans 1961)

$$a(m_J + m) = C \quad (5)$$

where m is the satellite mass and C is a constant. Depending on the exact timing of capture relative to Jupiter's exponential growth, it is clear from Eq. (5) that satellite orbits could be reduced in size by a considerable factor, leading to permanent capture. One appeal of "pull-down" capture is that the same mechanism might also stabilise the Trojans at $L4$ and $L5$, as we later discuss. One potential problem with "pull-down" is that Jupiter formation might occur so rapidly that no macroscopic bodies would have time to grow before Jupiter reached full mass. Proto-gas-giant clumps in the disk instability model of Boss (2001), for instance, have free fall times of 1 yr, too short for solid bodies to grow to 100 km scale through collisional agglomeration. This would be less a problem if Jupiter grew by the slower core accretion process, in which the heavy-element core grows slowly (on 10^6 to 10^7 yr timescales) followed by a rapid growth to full mass from capture of nebular gas. In this case, the irregular satellites and the Trojans could be nearby solid bodies that escaped incorporation into the core and were later trapped by the envelope. Still another possibility is that the satellites were captured through a hybrid process: Lagrange point capture attended by Jupiter mass growth coupled with dissipation due to remnant planetary gas. Lastly, the data do not preclude the possibility that different satellites were captured through different processes. For example, the prograde satellites could have been trapped by libration-point capture and weak gas drag and the retrogrades by pull-down capture attended by both mass-growth and nebular drag. The problem of the origin of the irregulars is severely under-constrained.

The action of (weak) gas drag on the post-fragmentation satellites is consistent with the finding that some of these objects occupy resonances. In a 10^5 yr numerical integration of the motions of the satellites, Whipple and Shelus (1993) found a resonance between the longitude of perijove of JVIII Pasiphae and the longitude of perihelion of Jupiter, with a libration period of 13,500 years. JIX Sinope also locks intermittently in this same resonance and is additionally trapped in a 1:6 mean motion resonance (Saha and Tremaine 1993). The resonances, which act to protect the satellites from solar perturbations, occupy a small fraction of phase space suggesting that they are not populated by chance. Weak gas drag would drive slow orbital decay and allow trapping of some of the satellites in resonances, as is observed. Note that the required weak gas drag is qualitatively different from the strong gas drag invoked above to explain capture. Orbital evolution under the latter proceeds too rapidly for resonance trapping to occur. Weak drag could result from a tenuous gas atmosphere persisting after the hydrodynamic collapse of the planet. Capture into resonance could also be driven by late-stage, slow mass growth of Jupiter, with or without the assistance of weak drag (Saha and Tremaine 1993). Recent numerical orbital integrations (R. Jacobson, personal communication) suggest that one of the new jovian satellites, 2001J10, is a Kozai resonator. Its inclination, 145.8 deg, falls within the stable zone below the critical value of about 147 degrees found for the jovian retrograde group in numerical simulations (V. Carruba and M. Cuk, private communication).

In any case, given that capture after the formation epoch is unlikely, the existence of the irregular satellites and Trojans implies that sufficient time elapsed for 100 km and larger solid bodies to grow in the solar nebula near proto-Jupiter's orbit. This fits naturally with the "standard" model of gas giant planet formation, in which a rock/ice core grows to 5 - 10 $M_\oplus$ on timescales $\sim 10^7$ yr before precipitating gravitational instability and collapse of the surrounding gas nebula (Pollack et al. 1996). In this scenario, the irregular satellites and Trojans are pre-Jovian planetesimals that escaped both incorporation into the

body of Jupiter and ejection from the solar system by gravitational slingshot. Compositionally, they must be related to Jupiter's high molecular weight core but may be partially devolatilized by their continued exposure to the Sun. As remarked by Boss (2001) and others, the standard model has difficulty in forming Jupiter in the $\sim 10^6$ yr lifetime of the protoplanetary gas. Instead, Jupiter might have grown by coreless spontaneous gravitational collapse of the protoplanetary nebula on timescales possibly only $\sim 10^3$ yr (Boss 2001). It is hard to see how these models allow 100 km scale solid bodies, like those present in the irregular satellite and Trojan populations, to form fast enough to then be captured.

12.2.3 Collisional Lifetimes

The estimated collisional lifetimes of the irregular satellites in their present orbits are very long. As a result of their small size and large orbital separation, the timescale for satellite-satellite collisions is comparable to or longer than the age of the solar system (Kessler 1981). Collisions between the irregular satellites and short-period comets are also exceedingly rare. Statistically, there should have been no impacts of kilometer sized cometary nuclei with any of the irregular satellites in the entire age of the solar system (Nakamura and Yoshikawa 1995). These authors calculate that, if the cometary size distribution measured at diameters > 1 km can be extrapolated to diameters $\ll 1$ km, only ~ 1 collision will have occurred with a 70 meter or larger diameter nucleus, in the past 4.6 Gyr. Even allowing that this calculation is intrinsically uncertain, perhaps by an order of magnitude in impact flux, it is clear that the collisional lifetimes of the irregular satellites to cometary impact are very long. The existence of the dynamical groups (Figures 4 and 5) therefore implies that the fragmentation occurred early, either as part of the capture process or soon after it when the interplanetary projectile flux was many orders of magnitude higher than now.

Evidence for an on-going but very low rate of collisional production of dust from the satellites has been identified in data from the Galileo spacecraft impact detector by Krivov et al. 2002 (see also chapter by Kruger et al). They find prograde and retrograde micron-sized grains in the 50 R_J to 300 R_J radius range and suggest an origin by erosion of the satellites by the fluxes of interplanetary and interstellar dust. This dust orbits largely outside Jupiter's magnetosphere and so is dynamically influenced mostly by gravity (from Jupiter and the Sun) and radiation forces. The number density ($10\ km^{-3}$) is about 10 times the value in the local interplanetary medium, but far too small to permit optical detection.

12.3 THE TEMPORARY SATELLITES

Backwards numerical integrations of the motions of Jupiter-family comets show frequent involvement with, and occasional temporary captures by, Jupiter (Carusi and Valsecchi 1979, Carusi et al. 1985). For example, comets P/Gehrels 3, P/Oterma and P/Helin-Roman-Crockett have recently been trapped as temporary satellites while P/Smirnova-Chernykh, P/Gehrels 3 and P/Helin-Roman-Crockett are expected to become temporary satellites in the next century (Tancredi, Lindgren and Rickman 1990).

The most famous example of a temporarily captured object is D/Shoemaker-Levy 9 (hereafter SL9), which was a short-lived companion to the planet for several decades to a century before its demise in 1994 (Benner and McKinnon 1995, Kary and Dones 1996). If it had not collided with the planet, SL9 would have been eventually ejected by Jupiter, either to leave the solar system completely or to circulate amongst the planets as a short-period comet (or peculiar asteroid, depending on its volatile content).

In fact, comet P/Brooks 2 provides an excellent 19th Century example of a comet meeting the latter fate. It passed within $2R_J$ of Jupiter in July 1886 and, like SL9, was apparently tidally disrupted as a result (Sekanina and Yeomans 1985). The perihelion distance decreased from 5.45 AU before encounter to 1.94 AU afterwards. P/Brooks 2 was discovered 3 years after breakup as a multiple object, with up to 9 distinct components being reported. One fragment, perhaps ~ 0.8 km in diameter, survives to this day (Sekanina and Yeomans 1985).

These examples of temporary capture show the intimate involvement between Jupiter and the minor bodies of the solar system. We may thus envision a loose swarm of temporarily captured satellites in orbit about Jupiter. This swarm is distinct from the permanently captured irregulars in that its members change from decade to decade. A small steady-state population probably exists. The best empirical limits to this swarm (fewer than 210 members larger than 16 km in diameter) are not very tight and should be improved (Lindgren et al. 1996).

Object SL9 (Figure 9) is the best studied temporary satellite and merits special discussion here. The object was discovered in March 1993, after being broken up in July 1992 by tidal stresses induced in a close pass by Jupiter. Soon after discovery, the orbit was found to have perijove inside the body of the planet and a collision was accurately forecast. The longer-term motion of SL9 was highly chaotic (Lyapunov exponent $\gamma = 0.1\ yr^{-1}$, Benner and McKinnon 1995), preventing meaningful backwards integrations beyond $\sim$10 yrs before discovery. However, a consideration of the statistical nature of the orbits suggests that SL9 may have been orbiting Jupiter for up to 100 yrs prior to discovery (Benner and McKinnon 1995; Kary and Dones 1996). That it had escaped detection for so long demonstrates our lack of knowledge of the interloper population. Presumably, had it not broken up and consequently brightened by factors of hundreds due to the release of dust, SL9 would have remained undiscovered.

Figure 9: Comet D/Shoemaker-Levy 9, a temporary satellite of Jupiter, imaged on 17 May 1994 about 22 months after breakup and 2 months prior to impact with Jupiter. The string of fragments was at this time about 1.2×10^6 km ($17\ R_J$) in length. Image from Weaver et al. 1995.

Dynamical chaos makes it impossible to decide whether the pre-capture SL9 was a Jupiter-family comet, a Centaur

or (less likely) a Trojan or a main-belt asteroid. Spectral observations showed no gas in SL9, giving rise to speculation that it might have been an escaped asteroid. However, at heliocentric distances $R > 5$ AU, many comets appear devoid of coma and emit no measurable gas so these observations cannot be uniquely interpreted as showing an asteroidal nature. Substantial dust comae were observed around each of the fragments in SL9, however. In active comets, dust is expelled against nucleus gravity by drag forces due to gas released by sublimating ice. In SL9, in contrast, the bulk of the dust was produced by the break-up of the nucleus, and the comet as a whole underwent substantial fading with time, as the dust dissipated into circum-Jovian space (Jewitt 1995). Perhaps the best evidence for low-level outgassing (at $\sim 22\ kg\ s^{-1}$) is provided indirectly by the sustained circularity of the inner isophotes of the comae (Rettig and Hahn 1997). In the absence of resupply, these isophotes would become stretched by radiation pressure distortion and Keplerian shear.

The break-up of the nucleus by the small stresses induced by perijoval tides indicates that the nucleus must be weak (in tension). Models of gravitationally bound aggregates convincingly fit the astrometric data and suggest a parent body diameter $D \sim 1.5$ km and density $\rho \sim 500\ kg\ m^{-3}$ (Asphaug and Benz 1996). A globally weak structure could result from internal fractures produced by collisions or, in the cometary context, could result from agglomeration of constituent planetesimals (Weidenschilling 1997). Again, no definitive conclusions about the nature and origin of SL9 are possible based on photometric or spectroscopic observations but the data and model results are compatible with its being a cometary nucleus or small Centaur.

Figure 10: Impacts of SL9 on Jupiter taken UT 1994 Jul 21 at 06:50:03 at $2.3\mu m$ wavelength, where the disk of the planet appears dark due to strong methane absorption in the atmosphere. The bright object to the upper left is Io. The impact sites appear bright because they scatter sunlight at high altitudes above the methane.

The rate of impact of similarly sized bodies into Jupiter is uncertain, but can be estimated in several ways. The average time between collisions, T_c, obtained by integration of the motions of the known short-period comets is $T_c \sim 950$ yrs (Nakamura and Yoshikawa 1995). A similar exercise using a larger number of test particles to more fully sample the parameter space and correct for observational bias gives $30 \leq T_c \leq 500$ yrs for 1km nuclei, with a most probable value $T_c = 240$ yrs (Kary and Dones 1996).

Observations provide an independent estimate of the impact frequency. A search through the observational records for Jovian cloud markings that might be impact debris clouds (see Figure 10) has produced some interesting but not wholly convincing candidates (Hockey 1996). One of the most believable was recorded by the Italian-French astronomer Cassini in 1690 (Tabe, Watanabe and Jimbo 1997). It was observed over an 18 day period, during which its morphology evolved from round to elongated in a fashion consistent with stretching by the known zonal wind shear. The size of the feature suggests an impactor mass like that of SL9. If this is indeed an impact scar, an interval of $T_c \sim 300$ yrs for ~km sized comets is indicated.

Figure 11: Number of comets within a given perijove in the last 250 years, adapted from Kevin Zahnle (private communication). The orbits of Io and Europa are marked.

The impact timescale can also be observationally estimated from the number of close involvements between comets and Jupiter in modern history. Altogether, 5 cometary approaches to Jupiter with perijove distance $q_J \leq 3R_J$ have been recorded in the past 250 years (Zahnle, Dones and Levison 1998). Given that the number distribution of perijove distances is uniform in q_J, (i.e. the cumulative number of comets with $q_J \leq q$ is proportional to q, see Figure 11) this allows an estimate of the number of impacts with the planet. If 5 comets approach to within 3 R_J in 250 years, then the number reaching 1 R_J is 5/3 in 250 years, or a characteristic timescale between impacts of 150 years. This is an upper limit to the true timescale because only a fraction of the comets involved are likely to have been subsequently detected. In particular, comets scattered outwards by Jupiter are far less likely to be detected than those scattered towards the Sun. At face value, this effect alone would require an increase of the impact flux by a factor of two, and a reduction of the impact timescale to only 75 years.

Figure 12: Enki Catena on Ganymede, a ~150 km long chain of 13 craters thought to have been produced by the impact of a tidally split comet. Galileo image courtesy NASA.

Distinctive crater chains on the Galilean satellites Ganymede and Callisto provide still another constraint (Figure 12). Based on their peculiar morphology, these chains have been attributed to impacts by recently disrupted nuclei (Melosh and Schenk 1993). The limited range of lengths of the crater chains, from ~60 km to ~600 km (Schenk et al. 1996), restricts the interval between break-up and impact, basically requiring impact on the outbound leg of the orbit immediately following break-up. The fraction of disrupted comets that strike a satellite of radius r_s moving in an orbit of radius R_s is given, to within geometric factors near unity, by $(r_s/2R_s)^2$. The rate of formation of crater chains thus provides a direct measure of the rate of disruption of nuclei, which should be interpreted as the number of comets passing per unit time within the effective Roche radius (~2 R_J) of Jupiter's center. In this way, Schenk et al. (1996) find a mean disruption interval $\sim 550 \pm 225$ yrs for comets with diameters $D \geq 2$ km. Scaling for perijove distance (as $1/q_J$) and nucleus size (assuming a d^{-2} power law for the cumulative distribution of nucleus diameters) gives a mean interval for impacts of $D \geq 1$ km nuclei into Jupiter $T_c \approx 140 \pm 60$ yrs. The principal uncertainties in this estimate include the unmeasured ages of the surfaces of Ganymede and Callisto (assumed, based on crater counts, to be 4 Gyr

and 3.5 Gyr, respectively), and the scaling from crater chain dimensions to projectile size. Given that many of the numbers used in this calculation (e.g. the surface ages) are little more than guesses, it is remarkable that the timescale derived from the crater chains bears any resemblance to the timescale deduced by other methods: indeed, this is probably the most compelling evidence for the correctness of the crater chain formation model.

A reasonable conclusion from these estimates would be that kilometer sized comets strike Jupiter once every century. The corresponding average mass flux into the atmosphere is $dM/dt \sim 1000\ kg\ s^{-1}$ ($10^{-14}\ kg\ m^{-2}\ s^{-1}$), most of this in oxygen, silicon, carbon and heavier elements. The upper atmospheres of Jupiter (Lellouch et al 2002) and the other gas giant planets (Feuchtgruber et al. 1997) are known to contain H_2O, CO_2 and CO delivered from external sources. In Jupiter, the total mass flux from all sources needed to explain the upper atmospheric abundances of these oxygen bearing molecules is $dM/dt \sim 200\ kg\ s^{-1}$ ($3 \times 10^{-15}\ kg\ m^{-2}\ s^{-1}$) (Lellouch et al 2002 and see the chapter by Moses et al.). This is in good agreement with the flux estimated from SL9 type impactors, and suggests that comets are likely to be major contributors to this oxygen flux in the stratosphere.

Deeper in the atmosphere, a factor of 2 to 4 overabundance of metals relative to hydrogen has been recorded in Jupiter by the Galileo probe (Owen et al. 1999). When integrated over the 4.6 Gyr age of the solar system, the total mass delivered by comets is only $10^{-5}\ M_\oplus$. This is far too small to account for the measured overabundance in the deep atmosphere and a different source must be invoked.

Temporary captures of comets can also occur at the major mean motion resonances. For example, comets P/Whipple and P/Russell 3 recently occupied horseshoe orbits in 1:1 resonance with Jupiter, while P/Kowal-Vavrova was similarly trapped at the 4:3 resonance (Carusi et al. 1985). Knowledge of these captures has given rise to the idea that the Trojans, or some fraction of the Trojans, might consist of captured comets.

12.4 THE JOVIAN TROJANS

The leading (L4) and trailing (L5) Trojans share Jupiter's semi-major axis but are separated from Jupiter by about 60 degrees in orbital longitude (Figure 13). In the idealised planar, restricted three body (Sun-Jupiter-Trojan) approximation, these objects exhibit simple harmonic motion around the L4 and L5 Lagrangian points, described by

$$\frac{d^2\phi}{dt^2} + \left(\frac{27}{4}\right)\mu n_J^2 \phi = 0 \qquad (6)$$

where ϕ is the angular separation between the Trojan and the relevant Lagrangian point, t is time, μ is approximately the ratio of Jupiter's mass to that of the Sun and n_J is the mean motion (yr^{-1}) of Jupiter. This has the solution

$$\phi = \frac{A}{2} cos(\omega t + B) \qquad (7)$$

with A and B constants representing the amplitude and phase of the motion and angular frequency given by

$$\omega = \left(\frac{27}{4}\mu\right)^{1/2} n_J \qquad (8)$$

With $\mu \sim 0.001$, $n_J \sim 0.52\ yr^{-1}$, Equation (8) gives $\omega \sim 0.043\ yr^{-1}$, corresponding to a characteristic libration period $2\pi/\omega \sim 150$ yrs. The libration amplitudes of the various Trojans, A, are spread over a wide range with a mean near 30 deg. (Shoemaker et al. 1989, Milani 1993).

The known Trojans have been discovered in a variety of wide-field and other surveys. Unfortunately, many of these surveys are not well characterized in terms of areal extent and sensitivity; some even remain unpublished. For this reason, it is difficult to reliably reconstruct the intrinsic size and orbital element distributions from the apparent distributions (which are affected by observational selection). Therefore, the intrinsic properties of the Trojans as a group are less well known than might be expected from the size of the Trojan sample.

Figure 13: Plan view of the Jovian Trojans at epoch UT 2002 Jan 01. All numbered objects in the L4 (leading) and L5 (trailing) clouds are shown. The locations of L4 and L5 are marked, as is the orbit of Jupiter. A dashed circle shows the Hill sphere of Jupiter, to scale.

A classic example is provided by the relative numbers of L4 and L5 Trojans, which are often reported as $N4 > N5$ (e.g. Fleming and Hamilton 2000). It is true that, as of mid-1988, 105 of the known Trojans were in the L4 cloud while only 52 were in the L5 cloud ($N4/N5 \sim 2$; Shoemaker, Shoemaker and Wolf 1989) while a synthesis of Palomar Schmidt survey data suggested to van Houten et al. (1991) that $N4/N5 = 2$. However, as of February 2002, the IAU has assigned numbers (indicating that the orbits are confidently known) to 530 Trojans and lists another 685 Trojans that have been less well observed. The ratio of the numbers in the two clouds is $N4/N5 = 696/519 \sim 1.3$. The Trojan population is probably completely known for absolute magnitudes $H_V < 9.0$ to 9.5 (Jewitt, Trujillo and Luu 2000), corresponding to diameters $D \sim 84$ to 105 km. The population ratios at these limiting magnitudes are $N4/N5 = 14/13 \sim 1$ and $N4/N5 = 41/28 \sim 1.4$, respectively. Given that the best characterized (brightest) Trojans show the smallest deviations of $N4/N5$ from unity, it is reasonable to suppose that the larger values of this ratio are produced by observational bias in favor of one cloud over the other. Such a bias could result from unequal observational coverage of the $L4$ and $L5$ clouds, perhaps due to their placement with respect to the Milky Way, making the detection of faint Trojans more difficult in one cloud than in the other. A careful experiment to determine $N4/N5$ free of the effects of observational bias has yet to be reported and is urgently needed.

The differential size distribution of the L4 Trojans is given by

$$n_1(r)dr = 1.5 \times 10^6 r^{-3.0\pm0.3} dr \qquad (9)$$

for $2.2 \leq r \leq 20$ km and

$$n_2(r)dr = 3.5 \times 10^9 r^{-5.5\pm0.9} dr \qquad (10)$$

for $r \geq 42$ km, where r is the radius computed on the assumption that the albedo is $p_R = 0.04$ (Jewitt, Trujillo

and Luu 2000). A smooth interpolation is presumed to exist in the radius range $20 \leq r \leq 42$ km. Integration of these equations gives the total population of Trojans with $r \geq 1$ km as N(1km) $\sim 1.6 \times 10^5$. The number of main-belt asteroids with radius $r \geq 1$ km is about 2.7×10^5 (Ivezic et al. 2001), showing that the two populations are of the same order (c.f. Shoemaker et al. 1989). The break in the Trojan size distribution may indicate that the smaller objects (Eq. (9)) are collisionally produced fragments of a parent population whose size distribution is given by Eq (10). Observational incompleteness at the 1 km scale is extreme: > 99 % of these objects remain unobserved.

12.4.1 Binaries

One Trojan (617 Patroclus) has been found to be double (Merline et al. 2001) with the two components differing in brightness by only 0.2 mag (Figure 14). Based on a nominal 0.05 albedo, the primary and secondary have diameters 105 km and 95 km, respectively. The maximum projected separation reported to date is 0.21 arcsec, corresponding to ~650 km. For comparison, the radius of the Hill sphere of the primary (assuming density 1000 $kg\ m^{-3}$) is 35,000 km showing that the Patroclus binary is very tightly bound. The origin of the binary is unclear. Numerical simulations of collisional disruption using N-body codes do produce satellites, but not (so far) with mass ratios near unity (Michel et al. 2001). Determination of the orbit will, through Kepler's Law, yield the binary mass. If the sizes of the components can then be accurately measured, the physically more interesting mean density could also be found. The fraction of binary Trojans has not been measured but the identification of even one such object amongst the few surveyed at sufficiently high angular resolution implies that the fraction may be large. In this regard, it has been suggested that large object 624 Hektor could be a contact binary (Hartmann and Cruikshank 1978). Careful measurement of the number and properties of binaries among the Trojans will place strong constraints on the time-integrated collisional environment and on the formation process.

Figure 14: H band (1.6 μm) image of Trojan 617 Patroclus taken 2001 October 13 by W. Merline et al and showing the two components separated by 0.12 arcsec. Image acquired using the Gemini North Telescope and the Hokupaa University of Hawaii adaptive optics system.

12.4.2 Families

The search for dynamical families among the Trojans is more difficult than in the main asteroid belt. This is because the velocity dispersion is similar to that among the asteroids while the available orbital element phase space is considerably smaller. Families are thus proportionally more dispersed over the available phase space and so are more difficult to identify against the background of unrelated objects. In the limiting case, catastrophic collisions between Trojans can impart velocities that carry family members out of the Lagrangian populations.

Despite these difficulties, about a dozen dynamical families have been reported (Shoemaker et al 1989, Milani 1993). Perhaps the most convincing are those with the smallest relative velocities between the components and which were found by both Shoemaker et al (1989) and Milani (1993). These include the pairs 1583 Antilochus, 3801 Thrasymedes and 1437 Diomedes, 2920 Automedon, which have relative velocities of a few $\times 10$ m s^{-1}. On physical grounds, the velocity dispersion should be comparable to the escape velocity from the largest fragment in each collision, as is the case for these pairs.

The reported Trojan families are also much smaller, in terms of numbers of objects per family, than those in the main belt. Milani (1993) suggests 8 members of the largest (Menelaus) family, but the membership of only a fraction of these appears secure. This paucity of the Trojan families is presumably an artifact of the much smaller number of Trojans having well-determined orbits. Our knowledge of the Trojan families should increase dramatically as the sample of reliable orbital elements is enlarged.

12.4.3 Physical Properties

What is the physical nature of the Trojans? Thermal infrared and optical measurements yield a mean geometric albedo $p_V = 0.056 \pm 0.003$ (standard error on the mean of 32 objects), with the maximum reported value $p_V = 0.18 \pm 0.02$ (4709 Ennomos; Fernandez et al. 2003). Similarly low albedos are characteristic of the nuclei of comets (Fernandez et al. 2001), where they are presumed (but not yet rigorously demonstrated) to indicate organic, perhaps carbonized surface compositions.

The optical reflection spectra of Trojans are approximately linear with wavelength and can be conveniently described in terms of the normalized reflectivity gradient, S' [%/1000Å] (Jewitt and Luu 1990, Fitzsimmons et al. 1994). This is the rate of change of the reflectivity with respect to wavelength, normalized to the continuum height at some reference wavelength (often 5000 Å). Histograms of S' are shown in Figure 15. There, the Trojans (Jewitt and Luu 1990) are indistinguishable from the irregular satellites (Luu 1991, Rettig 2001) and cometary nuclei (Jewitt 2002) in terms of their optical spectra, consistent with the comet nucleus analogy. The neutral to reddish colors and low albedos of the Trojans are close to those of outer-belt asteroids, where the P and D spectral types are numerically dominant (Gradie, Chapman and Tedesco 1989). The color distributions of the satellites, Trojans and nuclei are significantly different from those of the reddish Kuiper Belt Objects, however. The transformation from KBO to comet nucleus probably involves the burial of distinctive ultra-red material (material having $S' \geq 25$ %/1000Å) on the KBOs by refractory debris ejected through outgassing (Jewitt 2002). Spectral observations of Trojans in the $1 \leq \lambda \leq 2.5 \mu m$ near-infrared have failed to show any of the bands characteristic of vibrational overtones and combination frequencies in common molecular bonds, such as OH, CH, NH (Luu, Jewitt and Cloutis 1994; Dumas,

Owen and Barucci 1998). The water bands at 1.5 μm and 2.0 μm are specifically absent, as is the deeper (but harder to observe) 3.0 μm band (Jones et al. 1990, Cruikshank et al. 2001). These observations are all consistent with a largely refractory surface composition, perhaps consisting of an organic material (to provide the low albedos) with a large C/H ratio (to explain the non-detection of the common molecular bonds). A suitable terrestrial analogue might be common charcoal, which is dark and spectrally featureless. However, it must be said that unique interpretations of featureless reflection spectra, frequently with modest signal-to-noise ratios, are impossible. Plausible non-organic compositions also fit the data (Cruikshank et al. 2001).

Figure 15: Distributions of normalized optical reflectivity gradients for (top to bottom) the irregular satellites of Jupiter (data from Rettig 2001), Trojans (Jewitt and Luu 1990), cometary nuclei (Jewitt 2002) and Kuiper Belt Objects (Jewitt and Luu 2001).

Remote measurements sample only the surface skin and reveal little about the bulk composition of the Trojans. As previously remarked (Jewitt and Luu 1990), the available data are compatible with ice-rich Trojan interiors buried beneath a thermally insulating skin (mantle) of refractory matter. This is exactly the stratigraphy inferred in the nuclei of comets, where buried ice sublimates only from exposed vents embedded in a low albedo mantle consisting of refractory debris. The Trojans, formed at or beyond the protoplanetary snow-line, could be dormant comets. The higher albedo of Ennomos (Fernandez et al. 2003) hints at the possibility of surface ice, perhaps exposed by a recent impact, although less exciting explanations are certainly possible.

If the Trojans really are planetesimals from the 5 AU region of the protoplanetary disk trapped in dynamically stable niches, then they form a potentially valuable complement to the nuclei of the comets. Most long period comets formed in the 20 - 30 AU region and were scattered to the Oort Cloud (their storage location) mainly by Uranus, Neptune and, to a lesser extent Saturn (Hahn and Malhotra 1999). The Oort Cloud contribution from Jupiter was small (few percent) as a result of its greater mass and large ejection velocity (most Jupiter scattered planetesimals were launched above the escape velocity from the solar system and are lost to the interstellar medium). Conversely, most Jupiter family comets originate in the Kuiper Belt and therefore sample the disk in the 30 - 50 AU region. In moving from the Trojans, to the long-period comets to the Jupiter family comets, we sample objects formed at 5 AU (temperatures $T \sim 150$ K), 20 - 30 AU ($60 \leq T \leq 75$ K) and 30 - 50 AU ($45 \leq T \leq 60$ K), respectively. A comet having compositional characteristics suggesting formation near Jupiter's orbit has been reported (Mumma et al 2001). Perhaps it is appropriate to think of this body as a close relation of the irregular satellites and Trojans.

How might the suspected volatile nature of the Trojans be observationally tested? In the absence of in-situ spacecraft investigation, we must rely on chance exposures of ice uncovered by impacts. The surface stability of water frost depends critically on the ice temperature and hence on the albedo. At Jupiter's distance, the equilibrium sublimation rate of freshly deposited water ice frost (albedo = 0.9) at the subsolar point (i.e. the warmest location) of a non-rotating Trojan body is $\sim 2 \times 10^{-18} kg\ m^{-2}\ s^{-1}$. Such a frost would sublimate less than 1 mm in the age of the solar system. The same ice darkened to an albedo 0.1 by an admixture of absorbing refractory particles ('dirt') would, in equilibrium, sublimate at $5 \times 10^{-7} kg\ m^{-2}\ s^{-1}$, corresponding to the loss of a 1 mm layer in $\sim$1 month. Dirty water ice would generate a weak gas coma that would be hard to detect given existing instrumentation, and which would be short-lived due to the rapid ($\sim 10^3$ yr) formation of a thermally insulating rubble mantle over the sublimating surface (Jewitt 2002). The extreme sensitivity of the sublimation rate to the albedo shows that highly reflective fresh ice exposed by impact, for example, could survive indefinitely against sublimation provided its albedo remained high. We imagine the formation of bright ray craters on the Trojans caused by impacts puncturing the surface mantle and excavating buried ice. The persistence of exposed ice would probably be limited by other effects, particularly impact gardening of the surface layers leading to mixing with dark refractory grains. But before being mixed with other material, the ice should be identifiable both spectroscopically and in accurate, rotationally resolved albedo measurements.

12.4.4 Capture of Trojans

We noted earlier that comets are sometimes temporarily captured into the Lagrangian clouds. Permanent capture would require the action of a dissipative force or an increase in the Jupiter: Sun mass ratio. Regarding the former, collisions with other Trojans and non-gravitational forces due to asymmetrical mass loss from the comets have both been suggested (Yoder 1979). Quantitatively, in the present epoch, neither mechanism seems plausible. The probability of collision within the Trojan clouds is currently too small to effect capture in the limited (~few orbit) period of temporary capture, and non-gravitational forces are so weak at 5 AU that only the smallest bodies could possibly be influenced by them. We consider it unlikely that the Trojans are comets captured by outgassing forces. On the other hand, in the early solar system the numbers of objects moving in Jupiter's orbit may have been very much larger than at present. Collisional damping of the velocity dispersion could have stabilized objects near the $L4$ and $L5$ points, leading to the in-situ accumulation of the Trojans. Solar nebular gas drag would not have impeded this process (Peale 1993).

With regard to the planetary mass, the high abundance of H and He in Jupiter requires that this planet formed quickly, prior to the dissipation of the surrounding gas nebula. Observations of nearby young stars suggest gas disk survival times measured in millions of years (e.g. Briceno et al. 2001) while the terminal, hydrodynamic collapse phase of Jupiter's growth probably occurred on timescales $\sim 10^3$ yr. Objects in heliocentric orbit near the L4 and L5 points in the presence of a growing Jupiter could, in analogy with the trapping of satellites (Heppenheimer and Porco 1977, Namouni 1999) find themselves trapped

by the rapidly strengthening gravitational potential caused by Jupiter's growth (Fleming and Hamilton 2000). Kozai's mechanism may have played a role in trapping nearby bodies into retrograde irregular satellite orbits (Marzari and Scholl 1998b).

Numerical experiments provide some support for this conjecture. With a Jovian growth timescale of 10^5 yrs the capture efficiency is high for heliocentric inclinations ≤ 20 deg and negligible for inclinations ≥ 40 deg (Marzari and Scholl 1998). This matches the intrinsic inclination distribution of the Trojans: the bias-corrected mean inclination has been independently measured as ~17 deg. (Shoemaker et al. 1989) and 13.7 ± 0.5 deg (Jewitt, Trujillo and Luu 2000). Only two numbered Trojans ((19844) 2000 ST317 and (12929) 1999 TZ1) have $i \geq 40$ deg. Small eccentricities are also highly favored by the capture process.

However, capture by mass-growth predicts a distribution of libration amplitudes that is much wider than the one observed. The real Trojans, with a median libration amplitude near 30 degrees, are more tightly bound to the L4 and L5 points than expected from this model (for which the modal libration amplitude is near 70 degrees). One possible explanation if, indeed, mass growth is the explanation for capture, is that collisional dissipation of energy after capture has lead to the progressive damping of the libration amplitudes (Marzari and Scholl 1998). In this scenario, the smallest (highest velocity) fragments produced by collisions would be selectively lost from the Trojan clouds, leading to a flattening of the size distribution (c.f. Eq (9)). Alternatively, the current population may reflect selective loss of the large amplitude Trojans: orbits with large libration amplitudes are less stable than those of small amplitude (Levison, Shoemaker and Shoemaker 1997).

A realistic treatment of capture by the mass growth of Jupiter must necessarily include planetary migration. This is because the growing Jupiter exchanges angular momentum with planetesimals and with the gas disk of the solar nebula, allowing its orbit size to change on the same timescale as its mass grows. The semi-major axes of the orbits of all the giant planets are thought to have been altered by such torques. Saturn, Uranus and Neptune migrated outwards: the resonant structure in the distribution of Kuiper Belt Objects provides evidence for the magnitude (5 - 7 AU) and the timescale (1 - 10 Myr) of the outward migration of Neptune (Hahn and Malhotra 1999). Massive Jupiter provided the ultimate source of the angular momentum and, in contrast to the other planets, its orbit shrank, perhaps by only a few × 0.1AU. Resonant structure in the main-belt asteroid distribution may attest to this inward motion (Liou and Malhotra 1997). Fleming and Hamilton (2000) show that adiabatic changes in Jupiter's mass and semi-major axis relate to the Trojan libration amplitude, A, through

$$\frac{A_f}{A_i} = \left(\frac{m_{Ji}}{m_{Jf}}\right)^{1/4} \left(\frac{a_{ai}}{a_{Jf}}\right)^{1/4} \qquad (11)$$

where subscript $'i'$ refers to the initial value and $'f'$ to the final value. The changes can be considered adiabatic if they occur on timescales much longer than the 150 yr libration period given by Eq. (6). An adiabatic inward migration of Jupiter at constant mass by 0.5 AU to $a_{Jf} = 5.2$ AU would increase the libration amplitudes by a modest 2%. Adiabatic growth of Jupiter from ~10 $M_\oplus$ core mass to 317 $M_\oplus$ final mass would lead to a reduction in the libration amplitudes by a factor of $A_f/A_i \sim 0.4$. Therefore, the effects of migration are minor relative to those caused by mass growth.

The significance of radial migration is that the planets may have passed through mean motion resonances that would destabilize the Trojans. The current orbital periods of Jupiter (11.87 yrs) and Saturn (29.45 yrs) fall in the ratio 2.48:1, very close to the mean motion resonance at 5:2 (this is sometimes oddly known as the "Great Inequality"). An inward displacement of the orbit of Jupiter by only 0.02 AU would cause these planets to fall exactly into the 5:2 resonance. Perturbations on the Trojans of a growing, migrating Jupiter have been modelled by Gomes (1998) and Michtchenko, Beauge and Roig (2001). Both find strong dynamical effects upon passage through mean-motion resonances due to dynamical chaos. For example, the timescale for ejection of Trojans when at the 5:2 commensurability is only $\sim 10^6$ years. Much more severe effects are experienced at the 2:1 commensurability (corresponding to a Jupiter located at 6.00 AU), for which the 10^3 yr Trojan ejection lifetime is scarcely longer than the characteristic libration period. If the Jovian Trojans are primordial, these results suggest that Jupiter and Saturn can have never passed through the 2:1 commensurability, and therefore that the separation of the orbits of these two planets, presently at 4.33 AU, has not changed by more than 1 AU (Michtchenko et al. 2001). This inference is compatible with the relative motions of the planets needed to explain resonant structure in the main asteroid belt (Liou and Malhotra 1997) and in the Kuiper Belt (Hahn and Malhotra 1999).

12.4.5 Trojan Stability

Trojans are currently lost from the L4 and L5 clouds by two main processes. The dominant loss is from collisional shattering and the ejection of fragments. Collisions can occur between Trojans (the relevant velocity dispersion is ~ 5 $km\ s^{-1}$), and between Trojans and interplanetary projectiles (mostly long-period comets, which impact at characteristic speeds near 15 $km\ s^{-1}$). In high velocity, catastrophic impacts, the secondary fragment ejection velocity varies inversely with fragment mass. Therefore, the net effect should be a depletion of the smaller Trojans relative to the large ones, corresponding to a flattening of the size distribution relative to the production function. The rate of loss of kilometer-sized and larger Trojans has been estimated at $dN/dt \sim 10^{-3} yr^{-1}$ (Marzari, Farinella and Vanzani 1995). Given that the current population with $r \geq 1$ km is $N \sim 1.6 \times 10^5$ (Jewitt, Trujillo and Luu 2000), this estimate would suggest that the small Trojans are continually replenished (presumably by collisional shattering of larger Trojans) on timescales $N/(dN/dt) \sim 160$ Myr. Secondly, Trojan orbits appear to be weakly chaotic, but the Lyapunov timescales are much longer than the collision time (few $\times 10^9$ yr; Levison, Shoemaker and Shoemaker 1997) and the resultant loss rates correspondingly small. However, loss through dynamical instability is independent of Trojan size, potentially allowing the escape of even the largest Trojans, while collisional ejection affects small Trojans most strongly.

Observational evidence for collisional processing of the

Trojans is apparent in the size distribution which shows a slope break near r ~30 km (Jewitt, Trujillo and Luu 2000). The larger objects may be primordial, the smaller ones are collisionally produced fragments of these parent bodies. Other evidence for a size dependence of the physical properties of the Trojans includes an optical color-diameter trend (Jewitt and Luu 1990, Fitzsimmons et al 1994) that may suggest the increasing prevalence of collisional fragments at smaller sizes. Lastly, the rotational lightcurve amplitudes of large Trojans statistically exceed those of small Trojans, possibly suggesting the smoothing action of collisions (Binzel and Sauter 1992).

Objects scattered out of the Trojan clouds can encounter Jupiter, to become temporarily involved with that planet before impact, or ejected from the planetary system, or injected into planet-crossing orbits (Marzari, Farinella and Vanzani 1995). Escaped Trojans are dynamically similar to Jupiter family comets (Rabe 1972, Marzari, Farinella and Vanzani 1995). Estimates of the total Trojan population, when compared with the flux of JFCs, suggest that the fraction of the JFCs that might be escaped Trojans is $< 10\%$ (Marzari, Farinella and Vanzani 1995, Jewitt, Trujillo and Luu 2000). As with the irregular satellites, escaped Trojans whose perijoves fall into the realm of the Galilean satellites are subject to quick removal by collision. The fraction of impact craters on the Galilean satellites that might be caused by escaped Trojans has been estimated to fall in the 1 % to 10 % range (Zahnle, Dones and Levison 1998), with the dominant impactors being Jupiter Family Comets derived from the Kuiper Belt. This fraction is highly uncertain, however, not least because the size distributions of the Trojans and, particularly, the nuclei of comets are not well determined. It is possible that escaped Trojans dominate the impactor flux into the satellites, particularly at smaller diameters where the comets are believed to be depleted relative to power law extrapolations from larger sizes.

12.5 LEADING QUESTIONS

The big questions concern the sources and sinks of the irregular and temporary satellites and the Trojan librators, and the variations in the populations of these bodies with time. In particular, we would like to know if the irregulars and the Trojans are remnants of much larger initial populations that have been depleted over time by collisional or other effects. We also hope to understand the relationship between the bodies discussed in this review, and the materials that are widely presumed to exist in Jupiter's high molecular weight core: are they samples of the same material? A better understanding of this latter issue might one day motivate spacecraft exploration of (and sample return from) the Trojans. As always, the big questions are unlikely to be easily answered, and so we list a set of related but smaller, observationally more tractable questions that will take us some way towards our goal.

- Do the irregular satellites and/or the Trojans possess ice-rich interiors? This is suggested by their presumed formation at or beyond the snow-line, but no relevant observational constraints on the composition have been established.

- What is the size distribution of the irregular satellites as a whole, and within the separate subgroups? Is there a measurable minimum size that would provide evidence for depletion of the smallest bodies by gas drag?

- What correlations, if any, exist between the orbital and physical parameters of the irregular satellites? Correlations are expected from gas drag (for example, the smallest satellites are more strongly affected by drag, and should have orbits smaller and less eccentric than their larger counterparts).

- What is the distribution of spectral (compositional) types among the irregulars and how does this relate to their presumed origin by fragmentation of a small number of precursor objects?

- What is the current population and what are the main sources of temporary satellites (both planet impactors and others)?

- What are the unbiased orbital element distributions of the temporary and irregular satellites? Unbiased distributions will provide the strongest information about capture mechanisms and evolutionary processes.

- What fraction of the Trojans is binary and what is the distribution of separations and masses among the components of these objects? How do they form and what constraints do the binaries place on the collisional history of the Trojans?

- What fraction of the Trojans belongs to identifiable dynamical families?

- Can we identify escaped Jovian Trojans amongst the near-Earth objects? Low albedo, spectrally reddish near-Earth objects are known. How can we determine which, if any, of these are former Trojans?

12.6 ACKNOWLEDGEMENTS

We thank Julie Moses for pointers about meteoric infall to Jupiter, Yan Fernandez and Toby Owen for comments on the paper. Bob Jacobson computed the orbital elements listed in Table 1. This work was supported by grants to DCJ from NASA.

12.7 REFERENCES

Asphaug, E., and Benz, W. (1996). Size, Density, and Structure of Comet Shoemaker-Levy 9 Inferred from the Physics of Tidal Breakup Authors. Icarus, 121, 225-248.

Barucci, A., Cruikshank, D., Mottola, S., and Lazzarin, M. (2003). Physical Properties of Trojan and Centaur Asteroids. Asteroids III, ed. W. Bottke, Univ. Az. Press, Tuscon, pp. 273-288.

Beauge, C., Roig, F., and Nesvorny, D. (2002). Effects

of Planetary Migration on Natural Satellites of the Outer Planets. Icarus, 158, 483-498.

Benner, L. and McKinnon, W. (1995). On the Orbital Evolution and Origin of Comet Shoemaker-Levy 9. Icarus, 118, 155.

Binzel, R. P., and Sauter, L. (1992). Icarus, 95, 222-238.

Boss, A. (2001). Gas Giant Protoplanet Formation: Disk Instability Models with Thermodynamics and Radiative Transfer. Ap. J., 563, 367-373.

Briceno, C., Vivas, K., Calvet, N., Hartmann, L., Pacheco, R., Herrera, D., Romero, L., Berlind, P., Snchez, G., Snyder, J. and Andrews, P. (2001). The CIDA-QUEST Large-Scale Survey of Orion OB1: Evidence for Rapid Disk Dissipation in a Dispersed Stellar Population. Science, 291, 93-97.

Brown, M. E. (2000). Near-Infrared Spectroscopy of Centaurs and Irregular Satellites. Astron. J., 119, 977-983.

Brown, R. H. and 20 others. (2002). Near-Infrared Spectroscopy of Himalia. LPSC XXXIII, No. 2001.

Brunini, A., and Melita, M. (2002). On the Accretion of Uranus and Neptune. MNRAS., 330, 184-186.

Bus, S. J. (1999). Compositional Structure in the Asteroid Belt: Results of a Spectroscopic Survey. PhD Thesis, MIT.

Carruba, V., Burns, J., Nicholson, P., and Gladman, B. (2002). On the Inclination Distribution of the Jovian Irregular Satellites. Icarus, 158, 434-449.

Carusi, A. and Valsecchi, G. (1979). Numerical Simulations of Close Encounters Between Jupiter and Minor Bodies. In Asteroids, editor T. Gehrels, Univ. Az. Press, Tucson, pp. 391-416.

Carusi, A., Kresak, L., Perozzi, E., and Valsecchi, G. (1985). Long Term Evolution of Short-Period Comets. Adam Hilger, Ltd., Bristol.

Columbo, G., and Franklin, F. A. (1971). On the Formation of the Outer Satellite Groups of Jupiter. Icarus, 30, 186-189.

Cruikshank, D. P. (1977). Radii and Albedos of Four Trojan Asteroids and Jovian Satellites 6 and 7. Icarus, 30, 224-230.

Cruikshank, D., Degewij, J., and Zellner, B. (1982). The Outer Satellites of Jupiter. In Satellites of Jupiter, ed. D. Morrison, Univ. Az. Press, Tucson, pp129-146.

Cruikshank, D. et al. (2001). Constraints on the Composition of Trojan Asteroid 624 Hektor, Icarus, 153, 348-360.

De Sanctis, M. C., Lazzarin, M., Barucci, M. A., Capria, M. T., and Coradini, A. (2000). Astron. Ap., 354, 1086-1090.

Degewij, J., Zellner, B.; Andersson, L. E. (1980). Photometric properties of outer planetary satellites. Icarus, 44, 520-540.

Dell'Oro, A., Paolicchi, P., Marzari, F., Dotto, E., and Vanzani, V. (1998). Trojan Collision Probability: A Statistical Approach. Astron. Ap., 339, 272-277.

Dohnanyi, J. 1969. J. Geophys. Res. 74, 2531-2554.

Dumas, C., Owen, T., and Barucci, A. (1998). Near-Infrared Spectroscopy of Low-Albedo Surfaces of the Solar System: Search for the Spectral Signature of Dark Matter. Icarus, 133, 221-232.

Fernandez, Y., Jewitt, D., and Sheppard, S. (2001). Low Albedos Among Extinct Comet Candidates. Ap. J. Lett., 553, 197-200.

Fernandez, Y., Sheppard, S. and Jewitt, D. (2003). The Albedo Distribution of Jovian Trojan Asteroids. Astron. J., in press.

Feuchtgruber, H., Lellouch, E., de Graauw, T., Bezard, B., Encrenaz, T., and Griffin, M. (1997). External Supply of Oxygen to the Atmospheres of the Giant Planets. Nature, 389, 159-162.

Fitzsimmons, A., Dahlgren, M., Lagerkvist, C.-I., Magnusson, P., and Williams, I.P. 1994. Astron. Ap., 282, 634-642

Fleming, H. J., and Hamilton, D. P. (2000). On the Origin of the Trojan Asteroids: Effects of Jupiter's Mass Accretion and Radial Migration. Icarus, 148, 479-493.

Fujiwara, A., Cerroni, P., Davis, D., Ryan, E., di Martino, M., Holsapple, K., and Housen, K. (1989). Experiments and Scaling Laws for Catastrophic collisions. In Asteroids II, eds. R. Binzel, T. Gehrels and M. Matthews, Univ. Az. Press, pp. 240-265.

Gehrels, T. (1977). Some Interrelations of Asteroids, Trojans, and Satellites. In Comets Asteroids Meteorites, edited by A. Delsemme, University of Toledo Press, Toledo, pp. 323-326.

Gladman, B., Kavelaars, J. J., Holman, M., Nicholson, P., Burns, J. A., Hergenrother, C. W., Petit, J. M., Marsden, B. G., Jacobson, R., Gray, W., and Grav, T. (2001). Discovery of 12 Satellites of Saturn Exhibiting Orbital Clustering. Nature, 412, 163-166.

Gladman, B., et al. (2000). The Discovery of Uranus XIX, XX and XXI. Icarus, 147, 320.

Gomes, R. S. (1998). Dynamical Effects of Planetary Migration on Primordial Trojan-Type Asteroids. Astron. J. 116, 2590-2597.

Gradie, J., Chapman, C., and Tedesco, E. (1989). Distribution of Taxonomic Classes and the Compositional Structure of the Asteroid Belt. In Asteroids II, eds. R. Binzel, T. Gehrels and M. Matthews, Univ. Arizona Press, Tucson. pp. 316-335.

Grav, T., Holman, M., Gladman, B., and Aksnes, K. (2003). Photometric Survey of the Irregular Satellites. Icarus, submitted.

Hahn, J., and Malhotra, R. (1999). Orbital Evolution of Planets Embedded in a Planetesimal Disk. A. J., 117, 3041-3053.

Hartmann, W. K., and Cruikshank, D. P. (1978). The Nature of Trojan Asteroid 624 Hektor. Icarus, 36, 353-366.

Henon, M. (1970). Numerical Exploration of the Restricted Problem: VI. Hill's Case: Non-Periodic Orbits. Astron. Ap., 9, 24-36.

Heppenheimer, T. A., and Porco, C. C. (1977). New Contributions to the Problem of Capture. Icarus, 30, 385-401.

Hockey, T. (1996). The search for historical impact sites on Jupiter. Planet. Space Sci., 44, 559-564.

Holman, M., and Wisdom, J. (1993). Dynamical stability in the outer solar system andthe delivery of short period comets. Astron. J., 105, 1987-1999

Holman, M., Kavelaars, J., Grav, T., Fraser, W., and Milisavljevic, D. (2003). IAU Circular No. 8047 (January 13).

Ivezic, Z. et al. (2001). Solar System Objects Observed in the Sloan Digital Sky Survey Commissioning Data. Astron. J., 122, 2749-2784.

Jacobson, R. A. (2000). The Orbits of the Outer Jovian Satellites. Astron. J., 120, 2679-2686.

Jarvis, K. S. et al. (2000). JVI Himalia: New Compositional Evidence and Interpretation for the Origin of Jupiter's Small Satellites. Icarus, 145, 445-453.

Jeans, J. (1961). Astronomy and Cosmogony. Dover, New York. pp 298-299.

Jewitt, D. (1995). Pre-Impact Observations of P/Shoemaker-Levy 9. Proceedings of the European SL-9/Jupiter Workshop, eds. R. West and H. Boehnhardt, European Southern Observatory Workshop Proceedings No. 52. pp. 1-5.

Jewitt, D. (2002). Cometary Nuclei: The Missing Ultra-Red Matter. Astron. J., 123, 1039-1049.

Jewitt, D., C., and Luu, J. X. (1990). CCD Spectra of Asteroids II. The Trojans as Spectral Analogues of Cometary Nuclei, Astron. J., 100, 933-944.

Jewitt, D. C., Trujillo, C., and Luu, J. X. (2000). Population and Size Distribution of Small Jovian Trojan Asteroids. Astron. J., 120, 1140-1147.

Jewitt, D. and Luu, J. (2001). Colors and Spectra of Kuiper Belt Objects. A. J., 122, 2099-2114.

Jones, T., Lebofsky, L., Lewis, J.,and Marley, M. (1990). The composition and origin of the C, P, and D asteroids - Water as a tracer of thermal evolution in the outer belt. Icarus 88, 172-192.

Kary, D., and Dones, L. (1996). Capture Statistics of Short-Period Comets: Implications for Comet D/Shoemaker-Levy 9. Icarus 121, 207-224.

Kessler, D. J. (1981). Derivation of the Collision Probability Between Orbiting Objects: The Lifetimes of Jupiter's Outer Moons. Icarus, 48, 39-48.

Kowal, C., Aksnes, K., Marsden, B. and Roemer, E. (1978). Thirteen Satellite of Jupiter. A. J., 80, 460-464.

Kozai, Y. (1962). Secular Perturbations on Satellites of High Inclination and Eccentricity. Astron. J., 67, 591-598.

Krivov, A. V., Wardinski, I., Spahn, F., Kruger,H. and Grun, E. (2002). Dust on the Outskirts of the Jovian System. Icarus 157, 436-455.

Kuchner, M. J., Reach, W. T., and Brown, M. E. (2000). A Search for Resonant Structures in the Zodiacal Cloud with COBE DIRBE: The Mars Wake and Jupiter's Trojan Clouds. Icarus, 145, 44-52.

Kuiper, G. (1956). On the Origin of the Satellites and the Trojans. Vistas in Astronomy 2, pp. 1631-1666. New York, Pergammon.

Kuiper, G. (1961). Limits of Completeness. In Planets and Satellites, eds. G. Kuiper and B. Middlehurst, Univ. Chicago Press, Chicago, pp. 575-592.

Leinhardt, Z., Richardson, D., and Quinn, T. (2000). Direct N-Body Simulations of Rubble Pile Collisions. Icarus, 146, 133-151.

Lellouch, E., Bezard, B., Moses, J., Davis, G., Drossart, P., Feuchtgruber, H., Bergin, E., Moreno, R. and Encrenaz, T. (2002). The Origin of Water and Carbon Dioxide in Jupiter's Stratosphere. Icarus, 159, 112-131.

Levison, H. F., Shoemaker, E. M. and Shoemaker, C. S. 1997. Nature 385, 42-44.

Lindgren, M., Tancredi, G., Lagerkvist, C., and Hernius, O. (1996). Searching for Comets Encountering Jupiter. Astron. Ap. Supp., 118, 293-301.

Liou, J.-C., and Malhotra, R. (1997). Depletion of the Outer Asteroid Belt. Science, 275, 375-377.

Luu, J. (1991). CCD Photometry and Spectroscopy of the Outer Jovian Satellites. Astron. J., 102, 1213-1225.

Luu, J. X., Jewitt, D. C., and Cloutis, E. (1994). Near Infrared Spectroscopy of Primitive Solar System Objects, Icarus, 109, 133-144.

Marzari, F., and Scholl, H. (1998a). Capture of Trojans by a Growing Proto-Jupiter. Icarus, 131, 41-51.

Marzari, F., and Scholl, H. (1998b). The Growth of Jupiter and Saturn and the Capture of Trojans. Astron. Ap., 339, 278-285.

Marzari, F., Farinella, P., and Vanzani, V. (1995). Are Trojan Collisional Families a Source for Short-Period Comets? Astron. Ap., 299, 267-276.

Marzari, F., and Scholl, H. (2000). The Role of Secular Resonances in the History of the Trojans. Icarus, 146, 232-239.

Melosh, J., and Schenk, P. (1993). Split Comets and the Origin of Crater Chains on Ganymede. Nature, 365, 731-733.

Merline, W., Close, L., Siegler, N., and Potter, D. (2001). S/2001 (17) 1. IAUC 7741 (October 29).

Michel, P., Benz, W., Tanga, P., and Richardson, D. (2001). Collisions and Gravitational Reaccumulation: Forming Asteroid Families and Satellites. Science, 294, 1696-1700.

Milani, A. (1993). The Trojan Asteroid Belt: Proper Elements, Stability, Chaos and Families. Celestial Mechanics and Dynamical Astronomy, 57, 59-94.

Mitchtenko, T. A., Beauge, C., and Roig, F. (2001). Planetary Migration and the Effects of Mean Motion Resonances on Jupiter's Trojan Asteroids. Astron. J., 122, 3485-3491.

Mumma, M., Dello Russo, N., DiSanti, M., Magee-Sauer, K., Novak, R., Brittain, S., Rettig, T., McLean, I., Reuter, D. C., and Xu, Li-H. (2001). Organic Composition of C/1999 S4 (LINEAR): A Comet Formed Near Jupiter? Science, 292, 1334-1339

Nakamura, T., and Yoshikawa, M. (1995). Close encounters and collisions of short-period comets with Jupiter and its satellites. Icarus, vol. 116, p. 113-130.

Namouni, F. (1999). Secular Interactions of Coorbiting Objects. Icarus, 237, 293-314.

Nesvorny, D., and Dones, L. (2002). How Long-Lived Are the Hypothetical Trojan Populations of Saturn, Uranus, and Neptune? Icarus, 160, 271-288.

Owen, T., Mahaffy, P., Niemann, H., Atreya, S., Donahue, T., Bar-Nun, A., and de Pater, I. (1999). A low-temperature origin for the planetesimals that formed Jupiter. Nature, 402, 269-270.

Peale, S. J. (1993). The Effect of the Nebula on the Trojan Precursors. Icarus, 106, 308.

Perrine, C. (1905). Discovery of a Sixth Satellite to Jupiter. PASP, 17, 22-23.

Pollack, J. B., Burns, J. A., and Tauber, M. E. (1979). Gas Drag in Primordial Circumplanetary Envelopes: A Mechanism for Satellite Capture. Icarus, 37, 587-611.

Pollack, J., Hubickyj, O., Bodenheimer, P., Lissauer, J., Podolak, M., and Greenzweig, Y. (1996). Icarus, 124, 62

Porco, C. et al. (2003). In preparation.

Rabe, E. (1954). The Trojans as Escaped Satellites of Jupiter. Astronomical Journal, 59, 433-438.

Rettig, T., and Hahn, J. (1997). Comet Shoemaker-

Levy 9: an active comet. Planetary and Space Science, 45, 1271-1277

Rettig, T., Walsh, K., and Consolmagno, G. (2001). Implied Evolutionary Differences of the Jovian Irregular Satellites from a BVR Color Survey. Icarus, 154, 313-320.

Saha, P., and Tremaine, S. (1993). Orbits of the Retrograde Jovian Satellites. Icarus, 106, 549-562.

Sekanina, Z., and Yeomans, D. (1985). Orbital motion, nucleus precession, and splitting of periodic Comet Brooks 2. Astronomical Journal 90, 1985, 2335-2352.

Schenk, P., Asphaug, E., McKinnon, W., Melosh, H., Weissman, P. (1996). Cometary Nuclei and Tidal Disruption: The Geologic Record of Crater Chains on Callisto and Ganymede. Icarus, 121, 249-274

Sheppard, S., Jewitt, D., Fernandez, Y., and Magnier, E. (2001). IAU Circular No. 7555 (January 5).

Sheppard, S., Jewitt, D., and Kleyna, J. (2002). IAU Circular No. 7900 (May 16).

Sheppard, S., and Jewitt, D. (2003). Nature, in press.

Shoemaker, E. M., Shoemaker, C. S. and Wolfe, R. F. 1989. Asteroids II, eds.Binzel, R.P., Gehrels, T. and Matthews, M. S., University of Arizona Press, Tucson, 487-523.

Smith, D. W., Johnson, P. E., and Shorthill, R. W. (1981). Spectrophotometry of J8, J9 and Four Trojan Asteroids from 0.32 to 1.05 m. Icarus, 46, 108-113.

Sykes, M. V., Nelson, B., Cutri, R. M., Kirkpatrick, D. J., Hurt, R. and Skrutskie, M. F. (2000). Near-Infrared Observations of the Outer Jovian Satellites. Icarus, 143, 371-375.

Tabe, I., Watanabe, J., and Jimbo, M. (1997). Discovery of a Possible Impact Spot on Jupiter Recorded in 1690. PASJ., 49, L1-L5.

Tancredi, G., Lindgren, M., and Rickman, H. (1990). Temporary satellite capture and orbital evolution of Comet P/Helin-Roman-Crockett. Astron. Ap. 239, 375-380.

Tanga, P., Cellino, A., Michel, P., Zappal, V., Paolicchi, P., and dell'Oro, A. (1999). On the Size Distribution of Asteroid Families: The Role of Geometry. Icarus, 141, Icarus, 65-78.

Tholen, D. J., and Zellner, B. (1984). Multicolor Photometry of Outer Jovian Satellites. Icarus, 58, 246-253.

Van Houten, C. J., van Houten-Groeneveld, I., Wisse-Schouten, M., Bardwell, C., and Green, W. E. (1991). The Second Palomar-Leiden Trojan Survey. Icarus, 91, 326-333.

Weaver, H. et al. (1995). The Hubble Space Telescope (HST) Observing Campaign on Comet Shoemaker-Levy 9. Science 267, 1282.

Weidenschilling, S. (1997). The Origin of Comets in the Solar Nebula: A Unified Model. Icarus, 127, 290-306

Weigert, P, Innanen, K., and Mikkola, S. The Stability of Quasi-Satellites in the Outer Solar System. Astron. J., 119, 1978-1984.

Whipple, A., and Shelus, P. (1993). A Secular Resonance Between Jupiter and Its Eighth Satellite? Icarus, 101. 265-271.

Wolf, M. (1906). Photographische Aufnahmen von kleinen Planeten. Astron. Nachr. 170, 353.

Yoder, C. (1979). Notes on the origin of the Trojan asteroids. Icarus, 40, 341-344.

Zahnle, K., Dones, L., Levison, H. (1998). Cratering Rates on the Galilean Satellites. Icarus, 136, 202-222.

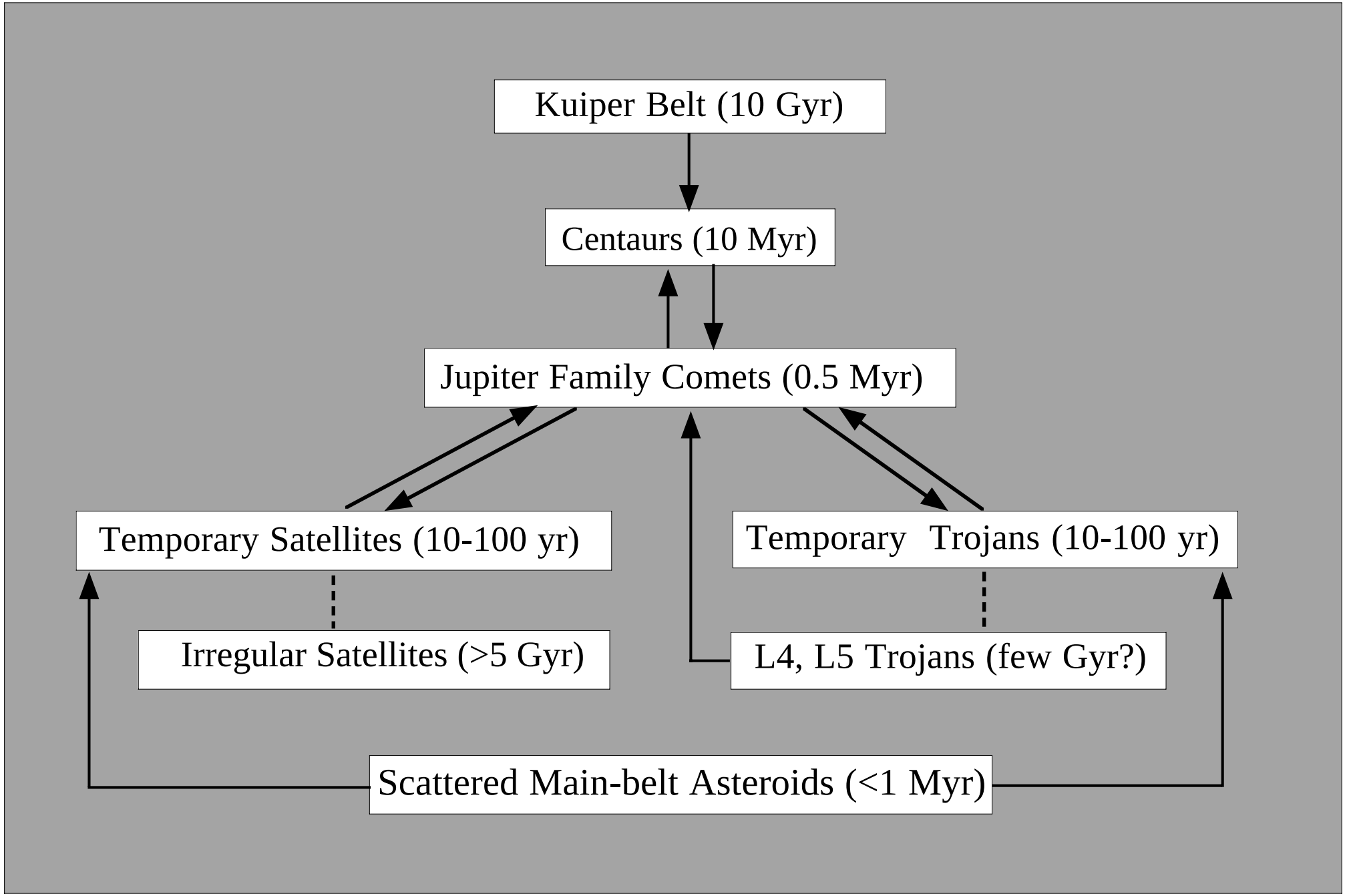
Kuiper Belt (10 Gyr)
Centaurs (10 Myr)
Jupiter Family Comets (0.5 Myr)
Temporary Satellites (10-100 yr)
Temporary Trojans (10-100 yr)
Irregular Satellites (>5 Gyr)
L4, L5 Trojans (few Gyr?)
Scattered Main-belt Asteroids (<1 Myr)

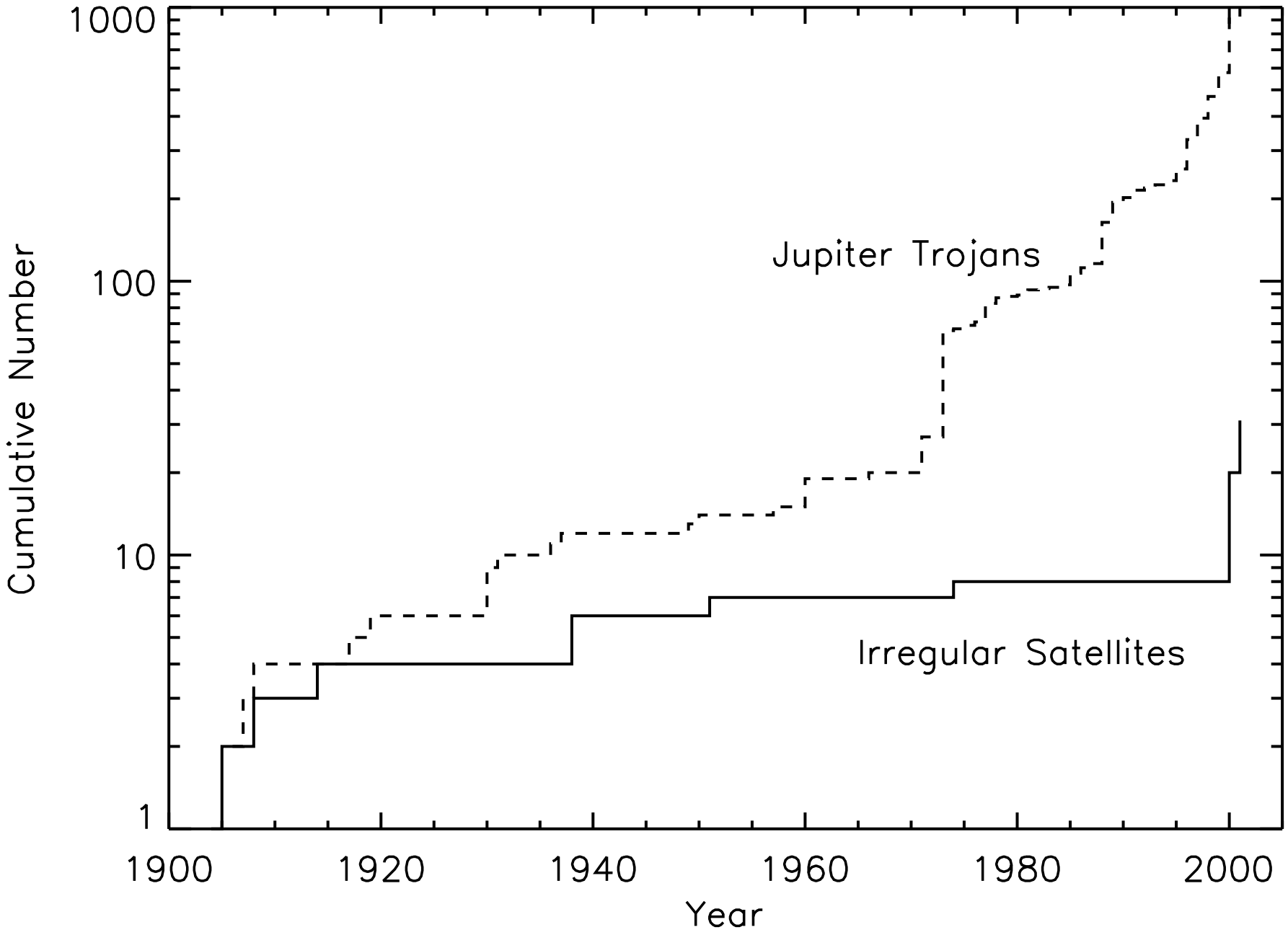
1000
100
10
1
Cumulative Number
Jupiter Trojans
Irregular Satellites
1900
1920
1940
1960
1980
2000
Year

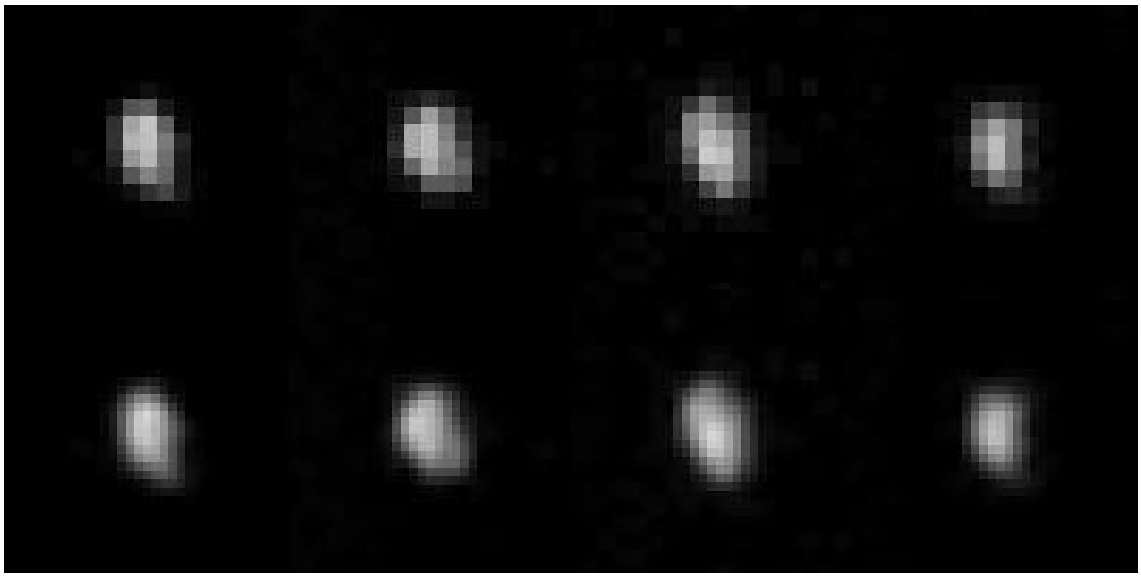

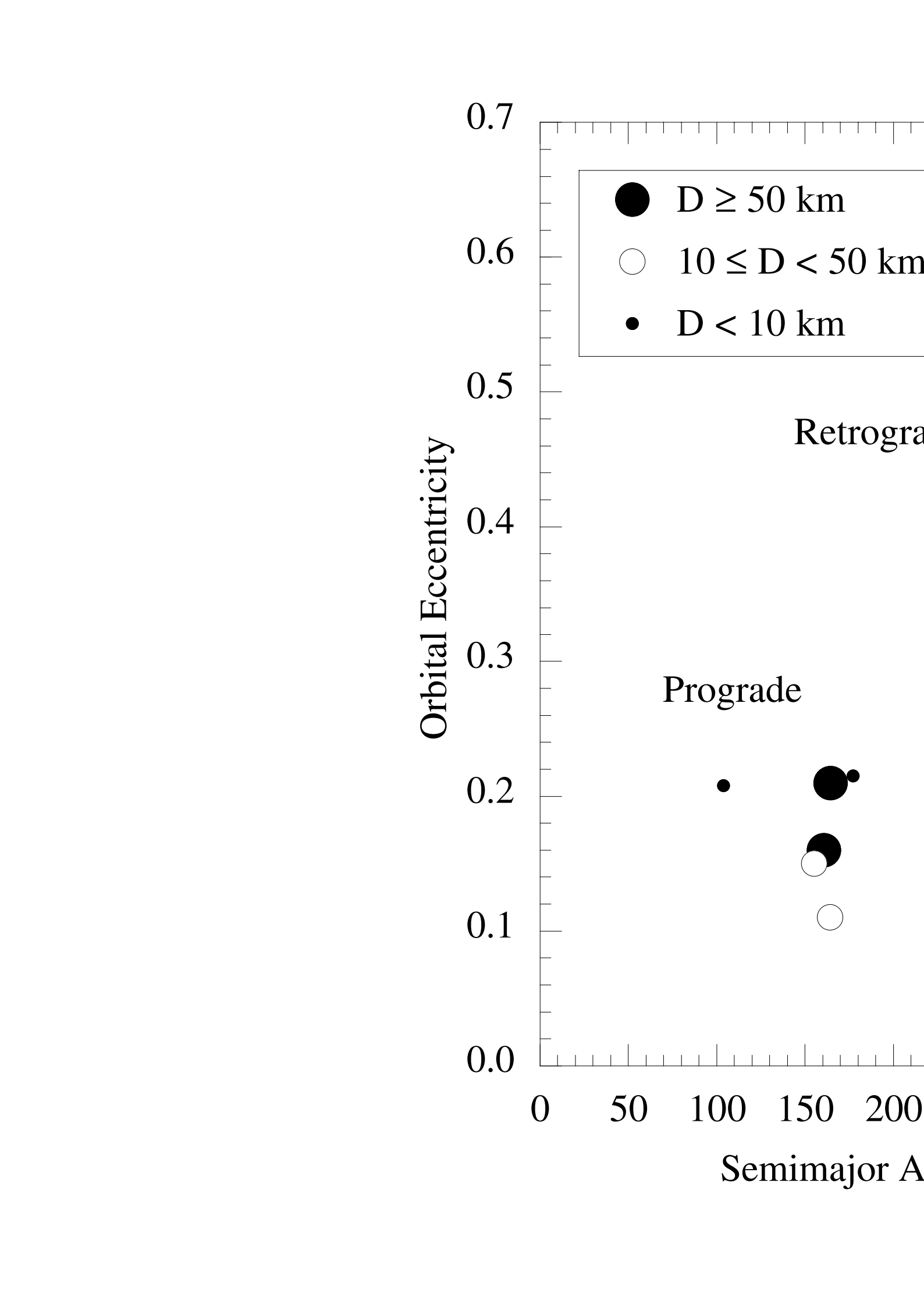
0.7
0.6
0.5
0.4
0.3
0.2
0.1
0.0
Orbital Eccentricity
D ≥ 50 km
10 ≤ D < 50 km
D < 10 km
Retrogra
Prograde
0
50
100
150
200
Semimajor A

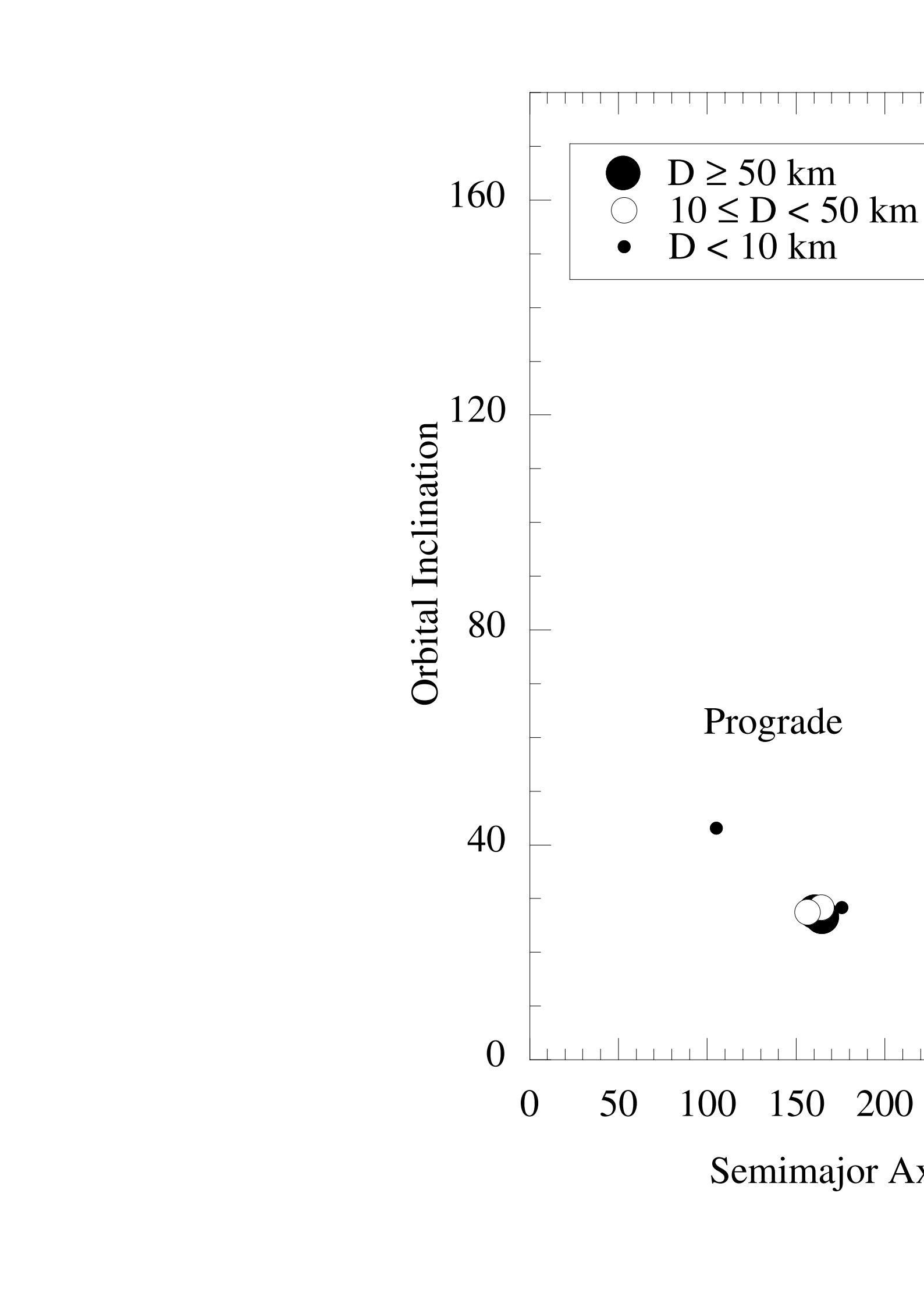
D ≥ 50 km
10 ≤ D < 50 km
D < 10 km
Orbital Inclination
160
120
80
40
0
Prograde
0
50
100
150
200
Semimajor Ax

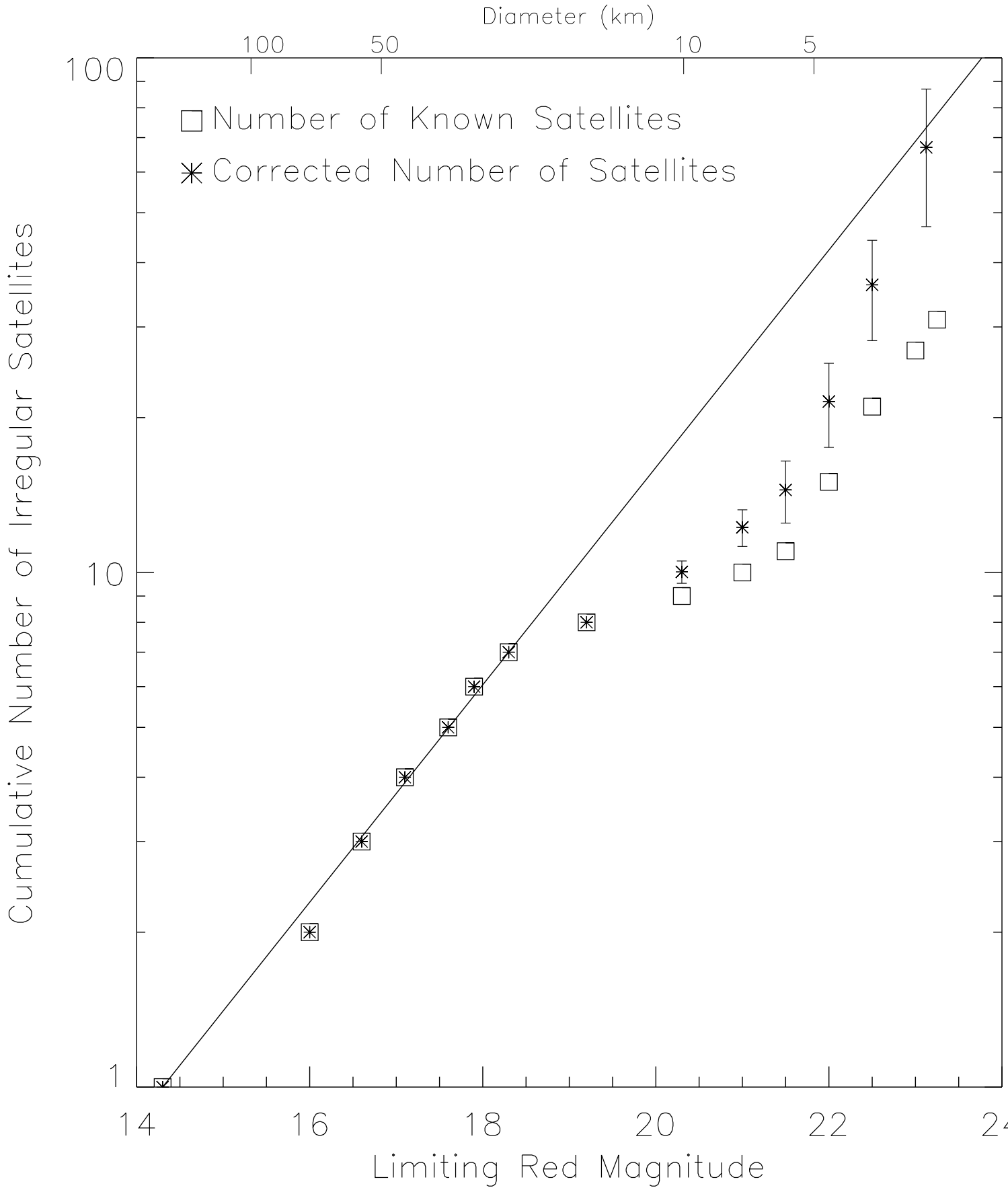
Diameter (km)
100
50
10
5
Number of Known Satellites
Corrected Number of Satellites
Cumulative Number of Irregular Satellites
100
10
1
14
16
18
20
22
24
Limiting Red Magnitude

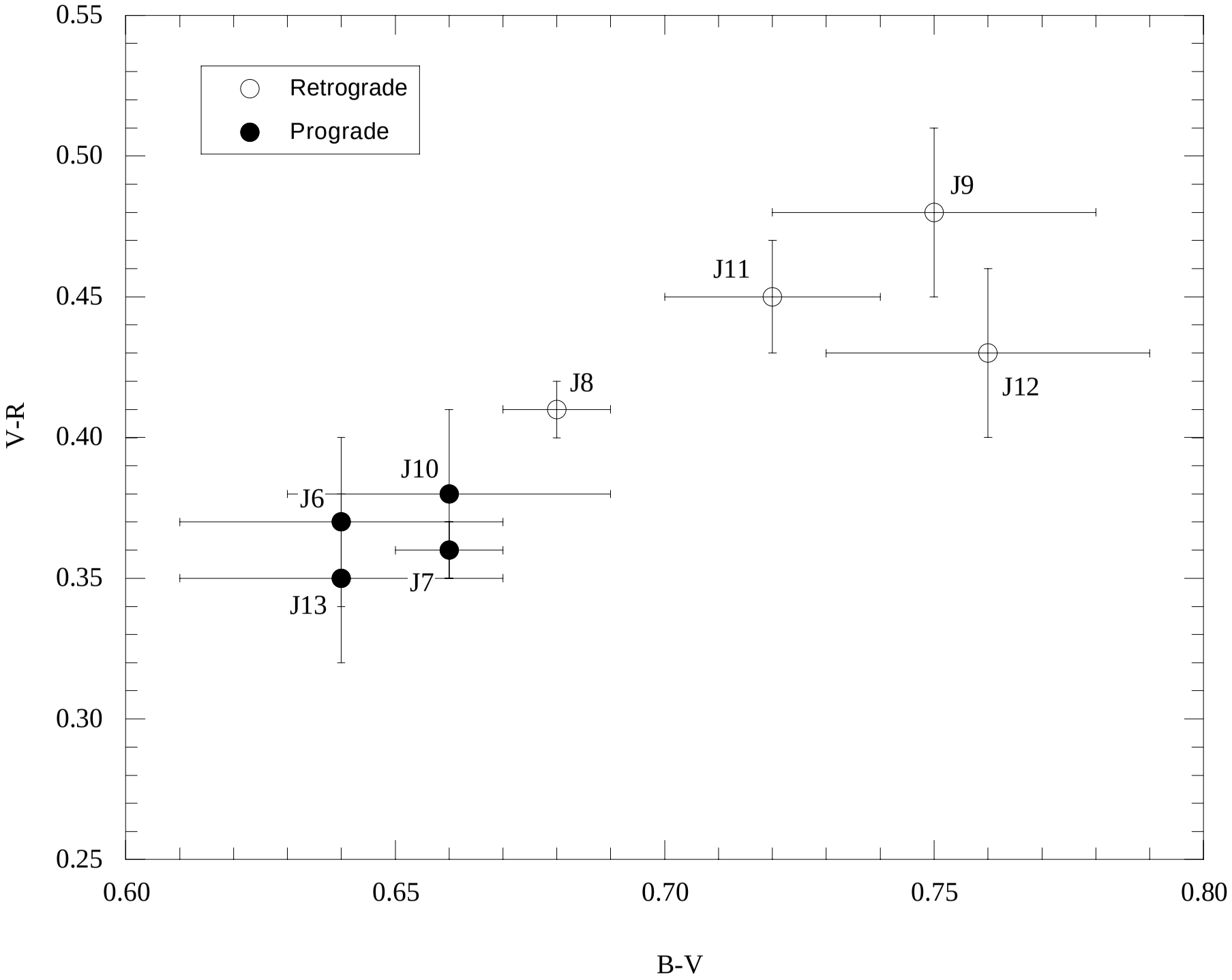
Retrograde
Prograde
J9
J11
J12
J8
J10
J6
J7
J13
V-R
B-V
0.55
0.50
0.45
0.40
0.35
0.30
0.25
0.60
0.65
0.70
0.75
0.80

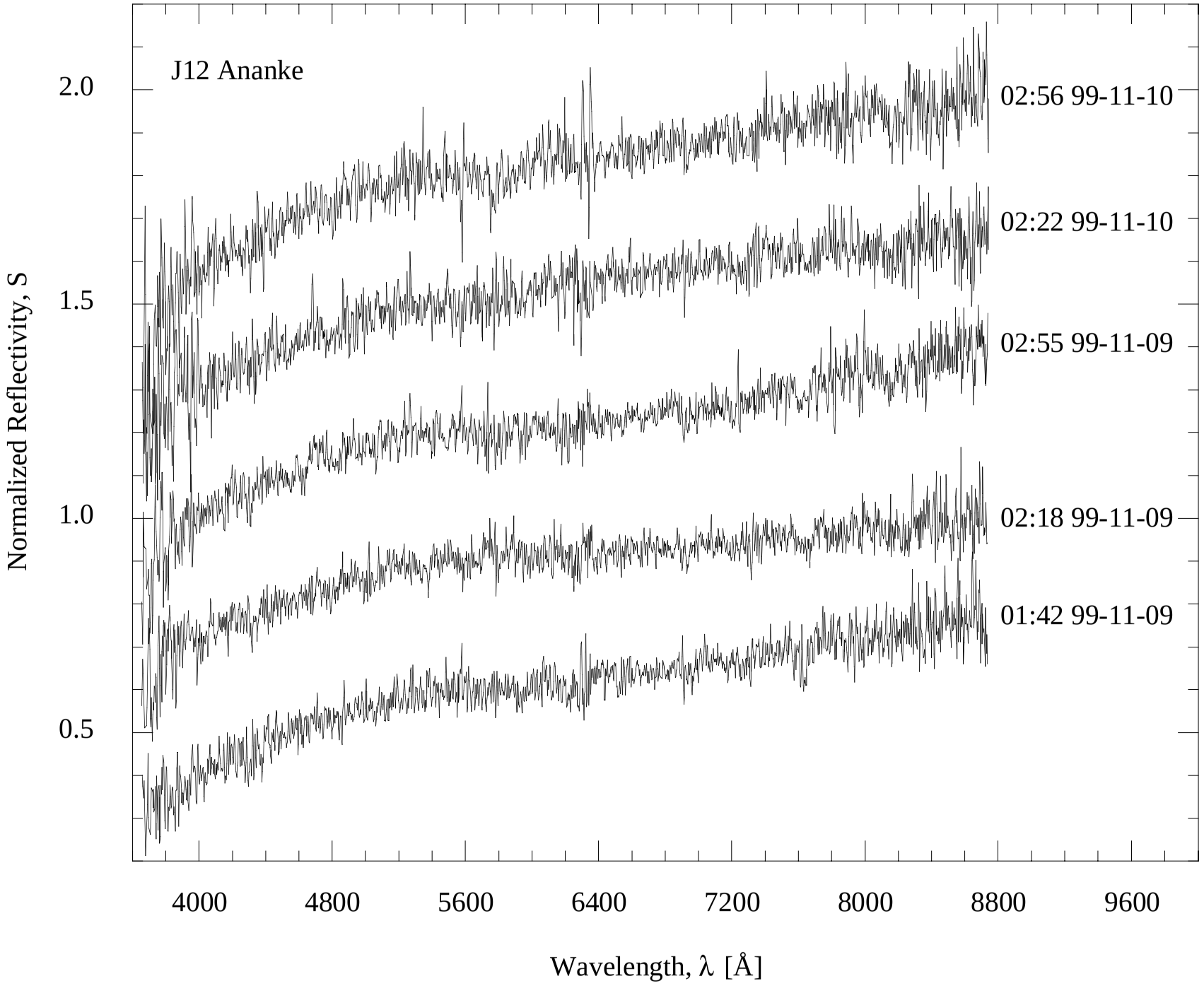
J12 Ananke
02:56 99-11-10
02:22 99-11-10
02:55 99-11-09
02:18 99-11-09
01:42 99-11-09
Normalized Reflectivity, S
2.0
1.5
1.0
0.5
4000
4800
5600
6400
7200
8000
8800
9600
Wavelength, λ [Å]

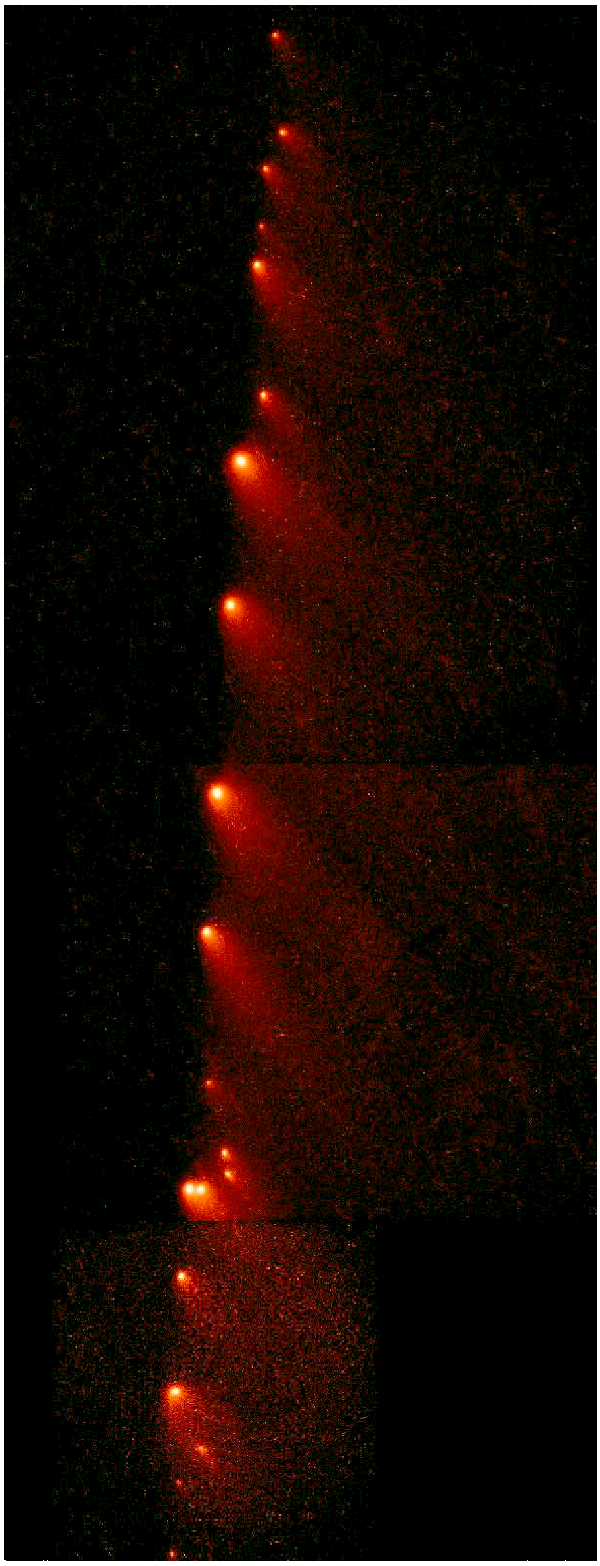


1024x1024 Near-Infrared Camera
University of Hawaii 2.2-meter telescope

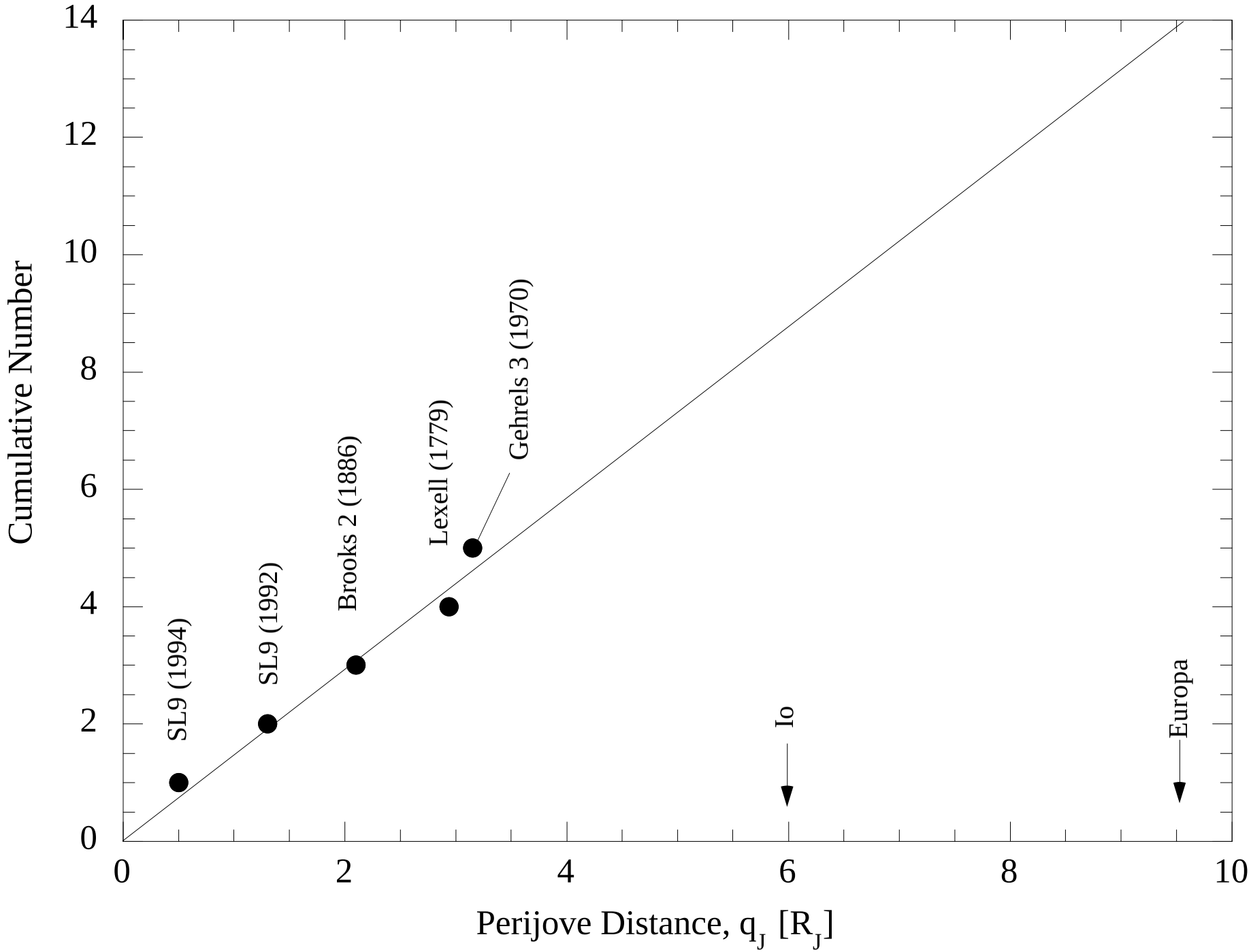
Cumulative Number
Perijove Distance, q_J [R_J]
0
2
4
6
8
10
12
14
SL9 (1994)
SL9 (1992)
Brooks 2 (1886)
Lexell (1779)
Gehrels 3 (1970)
Io
Europa

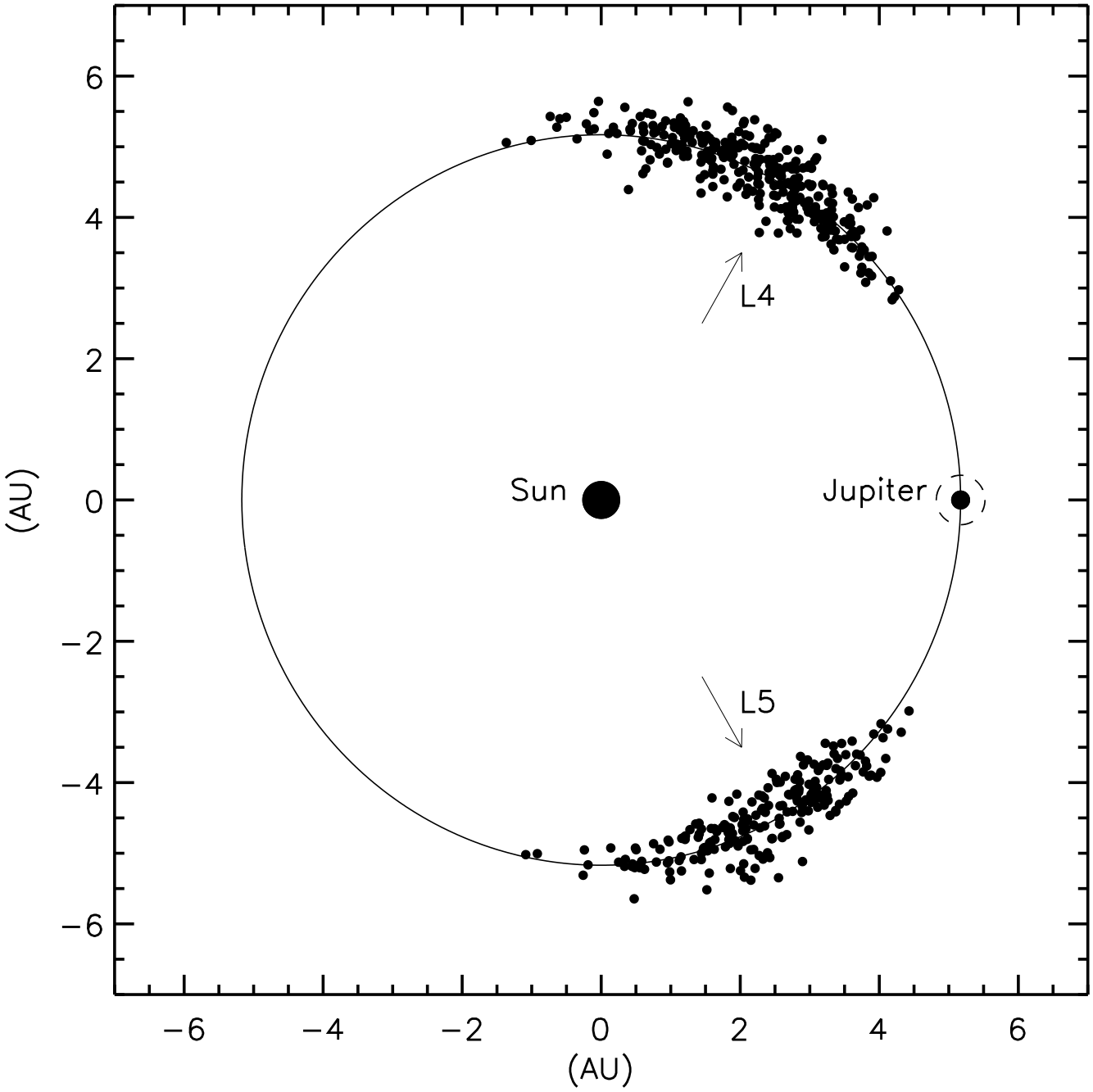
6
4
2
0
−2
−4
−6
(AU)
−6
−4
−2
0
2
4
6
(AU)
L4
L5
Sun
Jupiter

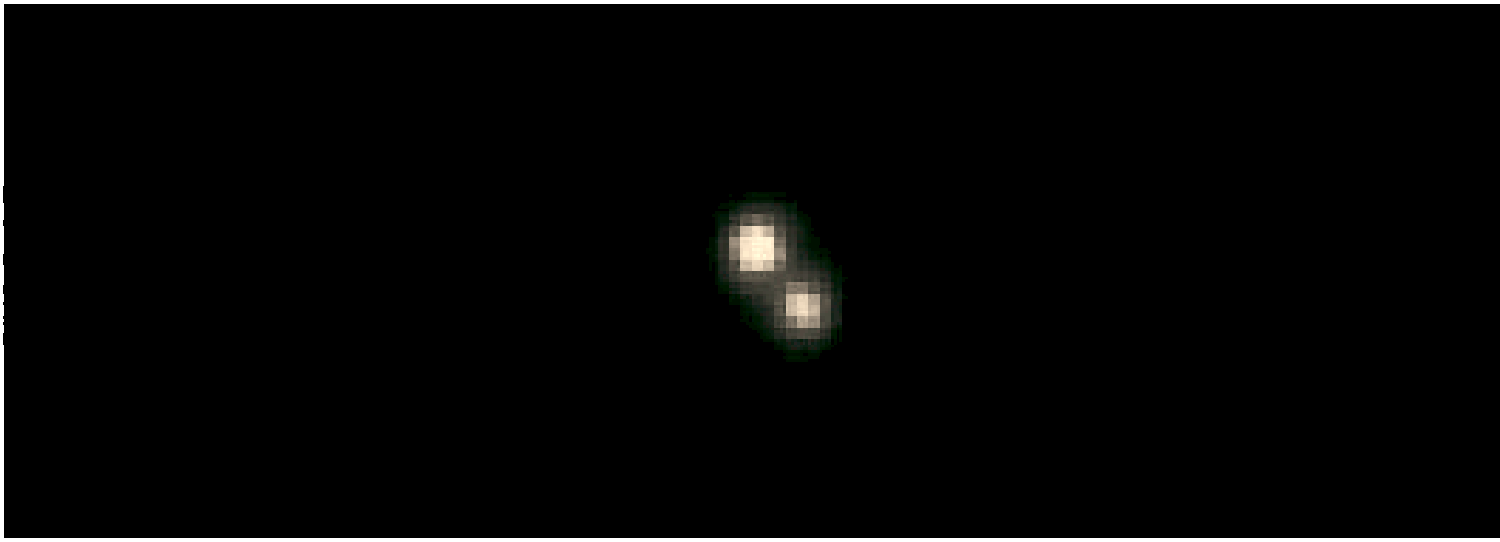

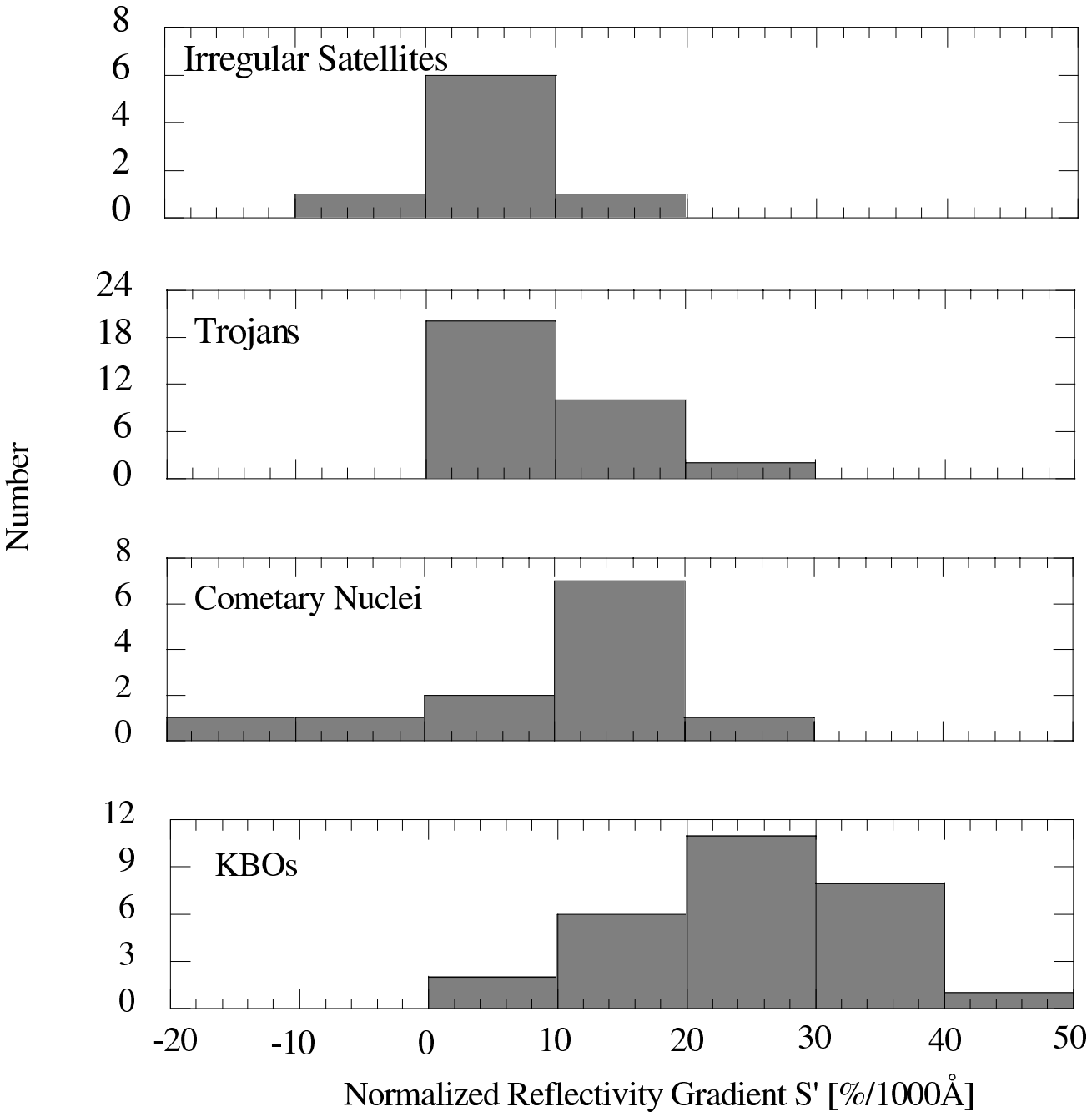
Irregular Satellites
Trojans
Cometary Nuclei
KBOs
Number
Normalized Reflectivity Gradient S' [%/1000Å]
-20
-10
0
10
20
30
40
50

TABLE 1. Physical and Orbital Properties of the Irregular Satellites*

Name	a[a] (km)	i[b] (deg)	e[c]	Peri[d] (deg)	Node[e] (deg)	M[f] (deg)	Period[g] (days)	mag.[h] (m_R)	H_R[i]	Diam.[j] (km)	Y
Themisto Group	Prograde										
XVIII Themisto	7507000	43.08	0.242	219.6	191.7	161.8	130.0	21.0	14.4	8	2
Himalia Group	Prograde										
XIII Leda	11165000	27.46	0.164	272.3	217.1	228.1	240.9	20.2	13.5	18	1
VI Himalia	11461000	27.50	0.162	332.0	57.2	68.7	250.6	14.8	8.1	184	1
X Lysithea	11717000	28.30	0.112	49.5	5.5	329.1	259.2	18.2	11.7	38	1
VII Elara	11741000	26.63	0.217	143.6	109.4	333.0	259.6	16.6	10.0	78	1
S/2000J11	12555000	28.27	0.248	184.8	290.3	309.9	287.0	22.4	16.1	4	2
Ananke Group	Retrograde										
S/2001J10	19394000	145.8	0.143	89.4	65.7	275.5	553.1	23.1	16.5	2	2
S/2001J7	21027000	148.9	0.230	325.0	261.4	114.1	620.0	22.8	16.2	3	2
XXII Harpalyke	21105000	148.6	0.226	140.6	37.2	351.7	623.3	22.2	15.2	4	2
XXVII Praxidike	21147000	149.0	0.230	196.3	287.6	251.8	625.3	21.2	15.0	7	2
S/2001J9	21168000	146.0	0.281	222.5	229.4	341.4	623.0	23.1	16.5	2	2
S/2001J3	21252000	150.7	0.212	308.0	338.3	258.5	631.9	22.1	15.5	4	2
XXIV Iocaste	21269000	149.4	0.216	68.4	276.8	345.8	631.5	21.8	14.5	5	2
XII Ananke	21276000	148.9	0.244	100.6	7.6	248.8	629.8	18.9	12.2	28	1
S/2001J2	21312000	148.5	0.228	100.4	240.8	14.5	632.4	22.3	15.7	4	2
Pasiphae Group	Retrograde										
S/2001J4	23219000	150.4	0.278	230.7	311.8	358.9	720.8	22.7	16.1	3	2
VIII Pasiphae	23624000	151.4	0.409	170.5	313.0	280.2	743.6	16.9	10.3	58	1
XIX Megaclite	23806000	152.8	0.421	287.8	286.8	189.7	752.8	21.7	15.0	6	2
S/2001J5	23808000	151.0	0.312	71.7	126.9	226.7	749.1	23.0	16.4	2	2
IX Sinope	23939000	158.1	0.250	346.4	303.1	168.4	758.9	18.3	11.6	38	1
XVII Callirrhoe	24102000	147.1	0.283	30.5	291.6	152.6	758.8	20.8	14.2	7	1
S/2001J1	24122000	152.4	0.319	58.5	279.7	192.0	765.1	22.0	15.4	4	2
Carme Group	Retrograde										
S/2001J6	23029000	165.1	0.267	242.3	336.6	279.2	716.3	23.2	16.6	2	2
S/2002J1	23064000	163.1	0.244	161.6	350.7	126.7	715.6	22.8	16.0	3	2
S/2001J8	23124000	165.0	0.267	53.3	68.7	274.8	720.9	23.0	16.4	2	2
XXI Chaldene	23179000	165.2	0.251	256.0	145.1	330.7	723.8	22.5	15.7	4	2
XXVI Isonoe	23217000	165.2	0.246	125.2	138.8	186.9	725.5	22.5	15.9	4	2
XXV Erinome	23279000	164.9	0.266	20.0	326.3	325.6	728.3	22.8	16.0	3	2
XX Taygete	23360000	165.2	0.252	239.9	312.8	154.1	732.2	21.9	15.4	5	2
XI Carme	23404000	164.9	0.253	28.2	113.7	234.0	734.2	17.9	11.3	46	1
S/2001J11	23547000	165.2	0.264	114.3	19.6	163.0	741.0	22.7	16.1	3	2
XXIII Kalyke	23583000	165.2	0.245	232.8	56.0	311.0	743.0	21.8	15.3	5	2

*Orbital data are from Robert Jacobson, Jet Propulsion Laboratory. Only satellites having well-determined orbit are listed.

[a]Mean orbital semi-major axis with respect to Jupiter.

[b]Mean inclination of orbit with respect to Jupiter's equator.

[c]Mean orbital eccentricity.

[d]Mean Argument of periapsis.

[e]Mean Longitude of ascending node.

[f]Mean anomaly of the orbit.

[g]Mean sidereal orbital period of satellite.

[h]Apparent red (0.65 micron wavelength) magnitude.

[i]Absolute magnitude of satellite if at zero phase angle and 1 AU from both the Earth and Sun.

[j]Diameter of satellite computed assuming a geometric albedo of 0.04.

[k]Year of the discovery.